Non-convex Statistical Optimization for Sparse Tensor Graphical Model

Wei Sun
Yahoo Labs
Sunnyvale, CA
sunweisurrey@yahoo-inc.com

Zhaoran Wang
Department of Operations Research
and Financial Engineering
Princeton University
Princeton, NJ
zhaoran@princeton.edu

Han Liu
Department of Operations Research
and Financial Engineering
Princeton University
Princeton, NJ
hanliu@princeton.edu

Guang Cheng
Department of Statistics
Purdue University
West Lafayette, IN
chengg@stat.purdue.edu

Abstract

We consider the estimation of sparse graphical models that characterize the dependency structure of high-dimensional tensor-valued data. To facilitate the estimation of the precision matrix corresponding to each way of the tensor, we assume the data follow a tensor normal distribution whose covariance has a Kronecker product structure. The penalized maximum likelihood estimation of this model involves minimizing a non-convex objective function. In spite of the non-convexity of this estimation problem, we prove that an alternating minimization algorithm, which iteratively estimates each sparse precision matrix while fixing the others, attains an estimator with the optimal statistical rate of convergence as well as consistent graph recovery. Notably, such an estimator achieves estimation consistency with only one tensor sample, which is unobserved in previous work. Our theoretical results are backed by thorough numerical studies.

1 Introduction

High-dimensional tensor-valued data are prevalent in many fields such as personalized recommendation systems and brain imaging research [1, 2]. Traditional recommendation systems are mainly based on the user-item matrix, whose entry denotes each user's preference for a particular item. To incorporate additional information into the analysis, such as the temporal behavior of users, we need to consider a user-item-time tensor. For another example, functional magnetic resonance imaging (fMRI) data can be viewed as a three way (third-order) tensor since it contains the brain measurements taken on different locations over time for various experimental conditions. Also, in the example of microarray study for aging [3], thousands of gene expression measurements are recorded on 16 tissue types on 40 mice with varying ages, which forms a four way gene-tissue-mouse-age tensor.

In this paper, we study the estimation of conditional independence structure within tensor data. For example, in the microarray study for aging we are interested in the dependency structure across different genes, tissues, ages and even mice. Assuming data are drawn from a tensor normal distribution, a straightforward way to estimate this structure is to vectorize the tensor and estimate the underlying Gaussian graphical model associated with the vector. Such an approach ignores the tensor structure

and requires estimating a rather high dimensional precision matrix with insufficient sample size. For instance, in the aforementioned fMRI application the sample size is one if we aim to estimate the dependency structure across different locations, time and experimental conditions. To address such a problem, a popular approach is to assume the covariance matrix of the tensor normal distribution is separable in the sense that it is the Kronecker product of small covariance matrices, each of which corresponds to one way of the tensor. Under this assumption, our goal is to estimate the precision matrix corresponding to each way of the tensor. See §1.1 for a detailed survey of previous work.

Despite the fact that the assumption of the Kronecker product structure of covariance makes the statistical model much more parsimonious, it poses significant challenges. In particular, the penalized negative log-likelihood function is non-convex with respect to the unknown sparse precision matrices. Consequently, there exists a gap between computational and statistical theory. More specifically, as we will show in §1.1, existing literature mostly focuses on establishing the existence of a local optimum that has desired statistical guarantees, rather than offering efficient algorithmic procedures that provably achieve the desired local optima. In contrast, we analyze an alternating minimization algorithm which iteratively minimizes the non-convex objective function with respect to each individual precision matrix while fixing the others. The established theoretical guarantees of the proposed algorithm are as follows. Suppose that we have n observations from a K-th order tensor normal distribution. We denote by m_k, s_k, d_k ($k = 1, \ldots, K$) the dimension, sparsity, and max number of non-zero entries in each row of the precision matrix corresponding to the k-th way of the tensor. Besides, we define $m = \prod_{k=1}^{K} m_k$. The k-th precision matrix estimator from our alternating minimization algorithm achieves a $\sqrt{m_k(m_k + s_k) \log m_k / (nm)}$ statistical rate of convergence in Frobenius norm, which is minimax-optimal since this is the best rate one can obtain even when the rest $K - 1$ true precision matrices are known [4]. Furthermore, under an extra irrepresentability condition, we establish a $\sqrt{m_k \log m_k / (nm)}$ rate of convergence in max norm, which is also optimal, and a $d_k \sqrt{m_k \log m_k / (nm)}$ rate of convergence in spectral norm. These estimation consistency results and a sufficiently large signal strength condition further imply the model selection consistency of recovering all the edges. A notable implication of these results is that, when $K \geq 3$, our alternating minimization algorithm can achieve estimation consistency in Frobenius norm even if we only have access to one tensor sample, which is often the case in practice. This phenomenon is unobserved in previous work. Finally, we conduct extensive experiments to evaluate the numerical performance of the proposed alternating minimization method. Under the guidance of theory, we propose a way to significantly accelerate the algorithm without sacrificing the statistical accuracy.

1.1 Related work and our contribution

A special case of our sparse tensor graphical model when $K = 2$ is the sparse matrix graphical model, which is studied by [5–8]. In particular, [5] and [6] only establish the existence of a local optima with desired statistical guarantees. Meanwhile, [7] considers an algorithm that is similar to ours. However, the statistical rates of convergence obtained by [6, 7] are much slower than ours when $K = 2$. See Remark 3.6 in §3.1 for a detailed comparison. For $K = 2$, our statistical rate of convergence in Frobenius norm recovers the result of [5]. In other words, our theory confirms that the desired local optimum studied by [5] not only exists, but is also attainable by an efficient algorithm. In addition, for matrix graphical model, [8] establishes the statistical rates of convergence in spectral and Frobenius norms for the estimator attained by a similar algorithm. Their results achieve estimation consistency in spectral norm with only one matrix observation. However, their rate is slower than ours with $K = 2$. See Remark 3.11 in §3.2 for a detailed discussion. Furthermore, we allow K to increase and establish estimation consistency even in Frobenius norm for $n = 1$. Most importantly, all these results focus on matrix graphical model and can not handle the aforementioned motivating applications such as the gene-tissue-mouse-age tensor dataset.

In the context of sparse tensor graphical model with a general K, [9] shows the existence of a local optimum with desired rates, but does not prove whether there exists an efficient algorithm that provably attains such a local optimum. In contrast, we prove that our alternating minimization algorithm achieves an estimator with desired statistical rates. To achieve it, we apply a novel theoretical framework to separately consider the population and sample optimizers, and then establish the one-step convergence for the population optimizer (Theorem 3.1) and the optimal rate of convergence for the sample optimizer (Theorem 3.4). A new concentration result (Lemma B.1) is developed for this purpose, which is also of independent interest. Moreover, we establish additional theoretical

guarantees including the optimal rate of convergence in max norm, the estimation consistency in spectral norm, and the graph recovery consistency of the proposed sparse precision matrix estimator.

In addition to the literature on graphical models, our work is also closely related to a recent line of research on alternating minimization for non-convex optimization problems [10–13]. These existing results mostly focus on problems such as dictionary learning, phase retrieval and matrix decomposition. Hence, our statistical model and analysis are completely different from theirs. Also, our paper is related to a recent line of work on tensor decomposition. See, e.g., [14–17] and the references therein. Compared with them, our work focuses on the graphical model structure within tensor-valued data.

Notation: For a matrix $\mathbf{A} = (\mathbf{A}_{i,j}) \in \mathbb{R}^{d \times d}$, we denote $\|\mathbf{A}\|_\infty, \|\mathbf{A}\|_2, \|\mathbf{A}\|_F$ as its max, spectral, and Frobenius norm, respectively. We define $\|\mathbf{A}\|_{1,\text{off}} := \sum_{i \neq j} |\mathbf{A}_{i,j}|$ as its off-diagonal ℓ_1 norm and $\|\mathbf{A}\|_\infty := \max_i \sum_j |\mathbf{A}_{i,j}|$ as the maximum absolute row sum. Denote $\text{vec}(\mathbf{A})$ as the vectorization of $\mathbf{A}$ which stacks the columns of $\mathbf{A}$. Let $\text{tr}(\mathbf{A})$ be the trace of $\mathbf{A}$. For an index set $\mathbb{S} = \{(i,j), i, j \in \{1, \ldots, d\}\}$, we define $[\mathbf{A}]_{\mathbb{S}}$ as the matrix whose entry indexed by $(i,j) \in \mathbb{S}$ is equal to $\mathbf{A}_{i,j}$, and zero otherwise. We denote $\mathbb{1}_d$ as the identity matrix with dimension $d \times d$. Throughout this paper, we use $C, C_1, C_2, \ldots$ to denote generic absolute constants, whose values may vary from line to line.

2 Sparse tensor graphical model

2.1 Preliminary

We employ the tensor notations used by [18]. Throughout this paper, higher order tensors are denoted by boldface Euler script letters, e.g. $\mathcal{T}$. We consider a K-th order tensor $\mathcal{T} \in \mathbb{R}^{m_1 \times m_2 \times \cdots \times m_K}$. When $K = 1$ it reduces to a vector and when $K = 2$ it reduces to a matrix. The $(i_1, \ldots, i_K)$-th element of the tensor $\mathcal{T}$ is denoted to be $\mathcal{T}_{i_1, \ldots, i_K}$. Meanwhile, we define the vectorization of $\mathcal{T}$ as $\text{vec}(\mathcal{T}) := (\mathcal{T}_{1,1,\ldots,1}, \ldots, \mathcal{T}_{m_1,1,\ldots,1}, \ldots, \mathcal{T}_{1,m_2,\ldots,m_K}, \mathcal{T}_{m_1,m_2,\ldots,m_K})^\top \in \mathbb{R}^m$ with $m = \prod_k m_k$. In addition, we define the Frobenius norm of a tensor $\mathcal{T}$ as $\|\mathcal{T}\|_F := \left(\sum_{i_1,\ldots,i_K} \mathcal{T}_{i_1,\ldots,i_K}^2 \right)^{1/2}$.

For tensors, a fiber refers to the higher order analogue of the row and column of matrices. A fiber is obtained by fixing all but one of the indices of the tensor, e.g., the mode-k fiber of $\mathcal{T}_{(k)}$ is given by $\mathcal{T}_{i_1,\ldots,i_{k-1},:,i_{k+1},\ldots,i_K}$. Matricization, also known as unfolding, is the process to transform a tensor into a matrix. We denote $\mathcal{T}_{(k)}$ as the mode-k matricization of a tensor $\mathcal{T}$, which arranges the mode-k fibers to be the columns of the resulting matrix. Another useful operation in tensors is the k-mode product. The k-mode product of a tensor $\mathcal{T} \in \mathbb{R}^{m_1 \times m_2 \times \cdots \times m_K}$ with a matrix $\mathbf{A} \in \mathbb{R}^{J \times m_k}$ is denoted as $\mathcal{T} \times_k \mathbf{A}$ and is of the size $m_1 \times \cdots \times m_{k-1} \times J \times m_{k+1} \times \cdots \times m_K$. Its entry is defined as $(\mathcal{T} \times_k \mathbf{A})_{i_1,\ldots,i_{k-1},j,i_{k+1},\ldots,i_K} := \sum_{i_k=1}^{m_k} \mathcal{T}_{i_1,\ldots,i_K} \mathbf{A}_{j,i_k}$. In addition, for a list of matrices $\{\mathbf{A}_1, \ldots, \mathbf{A}_K\}$ with $\mathbf{A}_k \in \mathbb{R}^{m_k \times m_k}$, $k = 1, \ldots, K$, we define $\mathcal{T} \times \{\mathbf{A}_1, \ldots, \mathbf{A}_K\} := \mathcal{T} \times_1 \mathbf{A}_1 \times_2 \cdots \times_K \mathbf{A}_K$.

2.2 Model

A tensor $\mathcal{T} \in \mathbb{R}^{m_1 \times m_2 \times \cdots \times m_K}$ follows the tensor normal distribution with zero mean and covariance matrices $\boldsymbol{\Sigma}_1, \ldots, \boldsymbol{\Sigma}_K$, denoted as $\mathcal{T} \sim \text{TN}(\mathbf{0}; \boldsymbol{\Sigma}_1, \ldots, \boldsymbol{\Sigma}_K)$, if its probability density function is

$$p(\mathcal{T}|\boldsymbol{\Sigma}_1, \ldots, \boldsymbol{\Sigma}_K) = (2\pi)^{-m/2} \left\{ \prod_{k=1}^K |\boldsymbol{\Sigma}_k|^{-m/(2m_k)} \right\} \exp \left(-\|\mathcal{T} \times \boldsymbol{\Sigma}^{-1/2}\|_F^2/2 \right), \qquad (2.1)$$

where $m = \prod_{k=1}^K m_k$ and $\boldsymbol{\Sigma}^{-1/2} := \{\boldsymbol{\Sigma}_1^{-1/2}, \ldots, \boldsymbol{\Sigma}_K^{-1/2}\}$. When $K = 1$, this tensor normal distribution reduces to the vector normal distribution with zero mean and covariance $\boldsymbol{\Sigma}_1$. According to [9, 18], it can be shown that $\mathcal{T} \sim \text{TN}(\mathbf{0}; \boldsymbol{\Sigma}_1, \ldots, \boldsymbol{\Sigma}_K)$ if and only if $\text{vec}(\mathcal{T}) \sim \text{N}(\text{vec}(\mathbf{0}); \boldsymbol{\Sigma}_K \otimes \cdots \otimes \boldsymbol{\Sigma}_1)$, where $\text{vec}(\mathbf{0}) \in \mathbb{R}^m$ and $\otimes$ is the matrix Kronecker product.

We consider the parameter estimation for the tensor normal model. Assume that we observe independently and identically distributed tensor samples $\mathcal{T}_1, \ldots, \mathcal{T}_n$ from $\text{TN}(\mathbf{0}; \boldsymbol{\Sigma}_1^*, \ldots, \boldsymbol{\Sigma}_K^*)$. We aim to estimate the true covariance matrices $(\boldsymbol{\Sigma}_1^*, \ldots, \boldsymbol{\Sigma}_K^*)$ and their corresponding true precision matrices $(\boldsymbol{\Omega}_1^*, \ldots, \boldsymbol{\Omega}_K^*)$ where $\boldsymbol{\Omega}_k^* = \boldsymbol{\Sigma}_k^{*-1}$ $(k = 1, \ldots, K)$. To address the identifiability issue in the parameterization of the tensor normal distribution, we assume that $\|\boldsymbol{\Omega}_k^*\|_F = 1$ for $k = 1, \ldots, K$. This renormalization assumption does not change the graph structure of the original precision matrix.

A standard approach to estimate $\mathbf{\Omega}_k^*$, $k = 1, \ldots, K$, is to use the maximum likelihood method via (2.1). Up to a constant, the negative log-likelihood function of the tensor normal distribution is $\text{tr}[\mathbf{S}(\mathbf{\Omega}_K \otimes \cdots \otimes \mathbf{\Omega}_1)] - \sum_{k=1}^{K}(m/m_k) \log |\mathbf{\Omega}_k|$, where $\mathbf{S} := \frac{1}{n}\sum_{i=1}^{n} \text{vec}(\mathcal{T}_i)\text{vec}(\mathcal{T}_i)^\top$. To encourage the sparsity of each precision matrix in the high-dimensional scenario, we consider a penalized log-likelihood estimator, which is obtained by minimizing

$$q_n(\mathbf{\Omega}_1, \ldots, \mathbf{\Omega}_K) := \frac{1}{m}\text{tr}[\mathbf{S}(\mathbf{\Omega}_K \otimes \cdots \otimes \mathbf{\Omega}_1)] - \sum_{k=1}^{K} \frac{1}{m_k} \log |\mathbf{\Omega}_k| + \sum_{k=1}^{K} P_{\lambda_k}(\mathbf{\Omega}_k), \qquad (2.2)$$

where $P_{\lambda_k}(\cdot)$ is a penalty function indexed by the tuning parameter λ_k. In this paper, we focus on the lasso penalty [19], i.e., $P_{\lambda_k}(\mathbf{\Omega}_k) = \lambda_k \|\mathbf{\Omega}_k\|_{1,\text{off}}$. This estimation procedure applies similarly to a broad family of other penalty functions.

We name the penalized model from (2.2) as the sparse tensor graphical model. It reduces to the sparse vector graphical model [20, 21] when $K = 1$, and the sparse matrix graphical model [5–8] when $K = 2$. Our framework generalizes them to fulfill the demand of capturing the graphical structure of higher order tensor-valued data.

2.3 Estimation

This section introduces the estimation procedure for the sparse tensor graphical model. A computationally efficient algorithm is provided to estimate the precision matrix for each way of the tensor.

Recall that in (2.2), $q_n(\mathbf{\Omega}_1, \ldots, \mathbf{\Omega}_K)$ is jointly non-convex with respect to $\mathbf{\Omega}_1, \ldots, \mathbf{\Omega}_K$. Nevertheless, $q_n(\mathbf{\Omega}_1, \ldots, \mathbf{\Omega}_K)$ is a bi-convex problem since $q_n(\mathbf{\Omega}_1, \ldots, \mathbf{\Omega}_K)$ is convex in $\mathbf{\Omega}_k$ when the rest $K - 1$ precision matrices are fixed. The bi-convex property plays a critical role in our algorithm construction and its theoretical analysis in §3.

According to its bi-convex property, we propose to solve this non-convex problem by alternatively update one precision matrix with other matrices fixed. Note that, for any $k = 1, \ldots, K$, minimizing (2.2) with respect to $\mathbf{\Omega}_k$ while fixing the rest $K - 1$ precision matrices is equivalent to minimizing

$$L(\mathbf{\Omega}_k) := \frac{1}{m_k}\text{tr}(\mathbf{S}_k \mathbf{\Omega}_k) - \frac{1}{m_k} \log |\mathbf{\Omega}_k| + \lambda_k \|\mathbf{\Omega}_k\|_{1,\text{off}}. \qquad (2.3)$$

Here $\mathbf{S}_k := \frac{m_k}{nm}\sum_{i=1}^{n} \mathbf{V}_i^k \mathbf{V}_i^{k\top}$, where $\mathbf{V}_i^k := \left[\mathcal{T}_i \times \left\{\mathbf{\Omega}_1^{1/2}, \ldots, \mathbf{\Omega}_{k-1}^{1/2}, \mathbb{1}_{m_k}, \mathbf{\Omega}_{k+1}^{1/2}, \ldots, \mathbf{\Omega}_K^{1/2}\right\}\right]_{(k)}$ with $\times$ the tensor product operation and $[\cdot]_{(k)}$ the mode-k matricization operation defined in §2.1. The result in (2.3) can be shown by noting that $\mathbf{V}_i^k = [\mathcal{T}_i]_{(k)}\left(\mathbf{\Omega}_K^{1/2} \otimes \cdots \otimes \mathbf{\Omega}_{k+1}^{1/2} \otimes \mathbf{\Omega}_{k-1}^{1/2} \otimes \cdots \otimes \mathbf{\Omega}_1^{1/2}\right)^\top$ according to the properties of mode-k matricization shown by [18]. Hereafter, we drop the superscript k of $\mathbf{V}_i^k$ if there is no confusion. Note that minimizing (2.3) corresponds to estimating vector-valued Gaussian graphical model and can be solved efficiently via the glasso algorithm [21].

Algorithm 1 Solve sparse tensor graphical model via Tensor lasso (Tlasso)

1: **Input:** Tensor samples $\mathcal{T}_1 \ldots, \mathcal{T}_n$, tuning parameters $\lambda_1, \ldots, \lambda_K$, max number of iterations T.
2: **Initialize** $\mathbf{\Omega}_1^{(0)}, \ldots, \mathbf{\Omega}_K^{(0)}$ randomly as symmetric and positive definite matrices and set $t = 0$.
3: **Repeat**:
4: $\quad t = t + 1$.
5: $\quad$**For** $k = 1, \ldots, K$:
6: $\qquad$ Given $\mathbf{\Omega}_1^{(t)}, \ldots, \mathbf{\Omega}_{k-1}^{(t)}, \mathbf{\Omega}_{k+1}^{(t-1)}, \ldots, \mathbf{\Omega}_K^{(t-1)}$, solve (2.3) for $\mathbf{\Omega}_k^{(t)}$ via glasso [21].
7: $\qquad$ Normalize $\mathbf{\Omega}_k^{(t)}$ such that $\|\mathbf{\Omega}_k^{(t)}\|_F = 1$.
8: $\quad$**End For**
9: **Until** $t = T$.
10: **Output:** $\widehat{\mathbf{\Omega}}_k = \mathbf{\Omega}_k^{(T)}$ $(k = 1, \ldots, K)$.

The details of our Tensor lasso (Tlasso) algorithm are shown in Algorithm 1. It starts with a random initialization and then alternatively updates each precision matrix until it converges. In §3, we will illustrate that the statistical properties of the obtained estimator are insensitive to the choice of the initialization (see the discussion following Theorem 3.5).

3 Theory of statistical optimization

We first prove the estimation errors in Frobenius norm, max norm, and spectral norm, and then provide the model selection consistency of our Tlasso estimator. We defer all the proofs to the appendix.

3.1 Estimation error in Frobenius norm

Based on the penalized log-likelihood in (2.2), we define the population log-likelihood function as

$$q(\boldsymbol{\Omega}_1, \ldots, \boldsymbol{\Omega}_K) := \frac{1}{m} \mathbb{E} \big\{ \mathrm{tr} \big[\mathrm{vec}(\mathcal{T}) \mathrm{vec}(\mathcal{T})^\top (\boldsymbol{\Omega}_K \otimes \cdots \otimes \boldsymbol{\Omega}_1) \big] \big\} - \sum_{k=1}^{K} \frac{1}{m_k} \log |\boldsymbol{\Omega}_k|. \quad (3.1)$$

By minimizing $q(\boldsymbol{\Omega}_1, \ldots, \boldsymbol{\Omega}_K)$ with respect to $\boldsymbol{\Omega}_k$, $k = 1, \ldots, K$, we obtain the population minimization function with the parameter $\boldsymbol{\Omega}_{[K]-k} := \{\boldsymbol{\Omega}_1, \ldots, \boldsymbol{\Omega}_{k-1}, \boldsymbol{\Omega}_{k+1}, \ldots, \boldsymbol{\Omega}_K\}$, i.e.,

$$M_k(\boldsymbol{\Omega}_{[K]-k}) := \operatorname*{argmin}_{\boldsymbol{\Omega}_k} q(\boldsymbol{\Omega}_1, \ldots, \boldsymbol{\Omega}_K). \quad (3.2)$$

Theorem 3.1. For any $k = 1, \ldots, K$, if $\boldsymbol{\Omega}_j$ $(j \neq k)$ satisfies $\mathrm{tr}(\boldsymbol{\Sigma}_j^* \boldsymbol{\Omega}_j) \neq 0$, then the population minimization function in (3.2) satisfies $M_k(\boldsymbol{\Omega}_{[K]-k}) = m \big[m_k \prod_{j \neq k} \mathrm{tr}(\boldsymbol{\Sigma}_j^* \boldsymbol{\Omega}_j) \big]^{-1} \boldsymbol{\Omega}_k^*$.

Theorem 3.1 shows a surprising phenomenon that the population minimization function recovers the true precision matrix up to a constant in only one iteration. If $\boldsymbol{\Omega}_j = \boldsymbol{\Omega}_j^*, j \neq k$, then $M_k(\boldsymbol{\Omega}_{[K]-k}) = \boldsymbol{\Omega}_k^*$. Otherwise, after a normalization such that $\|M_k(\boldsymbol{\Omega}_{[K]-k})\|_F = 1$, the normalized population minimization function still fully recovers $\boldsymbol{\Omega}_k^*$. This observation suggests that setting $T = 1$ in Algorithm 1 is sufficient. Such a suggestion will be further supported by our numeric results.

In practice, when (3.1) is unknown, we can approximate it via its sample version $q_n(\boldsymbol{\Omega}_1, \ldots, \boldsymbol{\Omega}_K)$ defined in (2.2), which gives rise to the statistical error in the estimation procedure. Analogously to (3.2), we define the sample-based minimization function with parameter $\boldsymbol{\Omega}_{[K]-k}$ as

$$\widehat{M}_k(\boldsymbol{\Omega}_{[K]-k}) := \operatorname*{argmin}_{\boldsymbol{\Omega}_k} q_n(\boldsymbol{\Omega}_1, \ldots, \boldsymbol{\Omega}_K). \quad (3.3)$$

In order to prove the estimation error, it remains to quantify the statistical error induced from finite samples. The following two regularity conditions are assumed for this purpose.

Condition 3.2 (Bounded Eigenvalues). For any $k = 1, \ldots, K$, there is a constant $C_1 > 0$ such that,

$$0 < C_1 \leq \lambda_{\min}(\boldsymbol{\Sigma}_k^*) \leq \lambda_{\max}(\boldsymbol{\Sigma}_k^*) \leq 1/C_1 < \infty,$$

where $\lambda_{\min}(\boldsymbol{\Sigma}_k^*)$ and $\lambda_{\max}(\boldsymbol{\Sigma}_k^*)$ refer to the minimal and maximal eigenvalue of $\boldsymbol{\Sigma}_k^*$, respectively.

Condition 3.2 requires the uniform boundedness of the eigenvalues of true covariance matrices $\boldsymbol{\Sigma}_k^*$. It has been commonly assumed in the graphical model literature [22].

Condition 3.3 (Tuning). For any $k = 1, \ldots, K$ and some constant $C_2 > 0$, the tuning parameter λ_k satisfies $1/C_2 \sqrt{\log m_k/(nmm_k)} \leq \lambda_k \leq C_2 \sqrt{\log m_k/(nmm_k)}$.

Condition 3.3 specifies the choice of the tuning parameters. In practice, a data-driven tuning procedure [23] can be performed to approximate the optimal choice of the tuning parameters.

Before characterizing the statistical error, we define a sparsity parameter for $\boldsymbol{\Omega}_k^*$, $k = 1, \ldots, K$. Let $\mathbb{S}_k := \{(i,j) : [\boldsymbol{\Omega}_k^*]_{i,j} \neq 0\}$. Denote the sparsity parameter $s_k := |\mathbb{S}_k| - m_k$, which is the number of nonzero entries in the off-diagonal component of $\boldsymbol{\Omega}_k^*$. For each $k = 1, \ldots, K$, we define $\mathbb{B}(\boldsymbol{\Omega}_k^*)$ as the set containing $\boldsymbol{\Omega}_k^*$ and its neighborhood for some sufficiently large constant radius $\alpha > 0$, i.e.,

$$\mathbb{B}(\boldsymbol{\Omega}_k^*) := \{\boldsymbol{\Omega} \in \mathbb{R}^{m_k \times m_k} : \boldsymbol{\Omega} = \boldsymbol{\Omega}^\top; \boldsymbol{\Omega} \succ 0; \|\boldsymbol{\Omega} - \boldsymbol{\Omega}_k^*\|_F \leq \alpha\}. \quad (3.4)$$

Theorem 3.4. Assume Conditions 3.2 and 3.3 hold. For any $k = 1, \ldots, K$, the statistical error of the sample-based minimization function defined in (3.3) satisfies that, for any fixed $\boldsymbol{\Omega}_j \in \mathbb{B}(\boldsymbol{\Omega}_j^*)$ $(j \neq k)$,

$$\big\| \widehat{M}_k(\boldsymbol{\Omega}_{[K]-k}) - M_k(\boldsymbol{\Omega}_{[K]-k}) \big\|_F = O_P \left(\sqrt{\frac{m_k(m_k + s_k) \log m_k}{nm}} \right), \quad (3.5)$$

where $M_k(\boldsymbol{\Omega}_{[K]-k})$ and $\widehat{M}_k(\boldsymbol{\Omega}_{[K]-k})$ are defined in (3.2) and (3.3), and $m = \prod_{k=1}^{K} m_k$.

Theorem 3.4 establishes the statistical error associated with $\widehat{M}_k(\mathbf{\Omega}_{[K]-k})$ for arbitrary $\mathbf{\Omega}_j \in \mathbb{B}(\mathbf{\Omega}_j^*)$ with $j \neq k$. In comparison, previous work on the existence of a local solution with desired statistical property only establishes theorems similar to Theorem 3.4 for $\mathbf{\Omega}_j = \mathbf{\Omega}_j^*$ with $j \neq k$. The extension to an arbitrary $\mathbf{\Omega}_j \in \mathbb{B}(\mathbf{\Omega}_j^*)$ involves non-trivial technical barriers. Particularly, we first establish the rate of convergence of the difference between a sample-based quadratic form with its expectation (Lemma B.1) via concentration of Lipschitz functions of Gaussian random variables [24]. This result is also of independent interest. We then carefully characterize the rate of convergence of $\mathbf{S}_k$ defined in (2.3) (Lemma B.2). Finally, we develop (3.5) using the results for vector-valued graphical models developed by [25].

According to Theorem 3.1 and Theorem 3.4, we obtain the rate of convergence of the Tlasso estimator in terms of Frobenius norm, which is our main result.

Theorem 3.5. Assume that Conditions 3.2 and 3.3 hold. For any $k = 1, \dots, K$, if the initialization satisfies $\mathbf{\Omega}_j^{(0)} \in \mathbb{B}(\mathbf{\Omega}_j^*)$ for any $j \neq k$, then the estimator $\widehat{\mathbf{\Omega}}_k$ from Algorithm 1 with $T = 1$ satisfies,

$$\|\widehat{\mathbf{\Omega}}_k - \mathbf{\Omega}_k^*\|_F = O_P\left(\sqrt{\frac{m_k(m_k + s_k)\log m_k}{nm}}\right), \tag{3.6}$$

where $m = \prod_{k=1}^K m_k$ and $\mathbb{B}(\mathbf{\Omega}_j^*)$ is defined in (3.4).

Theorem 3.5 suggests that as long as the initialization is within a constant distance to the truth, our Tlasso algorithm attains a consistent estimator after only one iteration. This initialization condition $\mathbf{\Omega}_j^{(0)} \in \mathbb{B}(\mathbf{\Omega}_j^*)$ trivially holds since for any $\mathbf{\Omega}_j^{(0)}$ that is positive definite and has unit Frobenius norm, we have $\|\mathbf{\Omega}_j^{(0)} - \mathbf{\Omega}_k^*\|_F \leq 2$ by noting that $\|\mathbf{\Omega}_k^*\|_F = 1$ $(k = 1, \dots, K)$ for the identifiability of the tensor normal distribution. In literature, [9] shows that there exists a local minimizer of (2.2) whose convergence rate can achieve (3.6). However, it is unknown if their algorithm can find such minimizer since there could be many other local minimizers.

A notable implication of Theorem 3.5 is that, when $K \geq 3$, the estimator from our Tlasso algorithm can achieve estimation consistency even if we only have access to one observation, i.e., $n = 1$, which is often the case in practice. To see it, suppose that $K = 3$ and $n = 1$. When the dimensions m_1, m_2, and m_3 are of the same order of magnitude and $s_k = O(m_k)$ for $k = 1, 2, 3$, all the three error rates corresponding to $k = 1, 2, 3$ in (3.6) converge to zero.

This result indicates that the estimation of the k-th precision matrix takes advantage of the information from the j-th way $(j \neq k)$ of the tensor data. Consider a simple case that $K = 2$ and one precision matrix $\mathbf{\Omega}_1^* = \mathbb{1}_{m_1}$ is known. In this scenario the rows of the matrix data are independent and hence the effective sample size for estimating $\mathbf{\Omega}_2^*$ is in fact nm_1. The optimality result for the vector-valued graphical model [4] implies that the optimal rate for estimating $\mathbf{\Omega}_2^*$ is $\sqrt{(m_2 + s_2)\log m_2/(nm_1)}$, which matches our result in (3.6). Therefore, the rate in (3.6) obtained by our Tlasso estimator is minimax-optimal since it is the best rate one can obtain even when $\mathbf{\Omega}_j^*$ $(j \neq k)$ are known. As far as we know, this phenomenon has not been discovered by any previous work in tensor graphical model.

Remark 3.6. For $K = 2$, our tensor graphical model reduces to matrix graphical model with Kronecker product covariance structure [5–8]. In this case, the rate of convergence of $\widehat{\mathbf{\Omega}}_1$ in (3.6) reduces to $\sqrt{(m_1 + s_1)\log m_1/(nm_2)}$, which is much faster than $\sqrt{m_2(m_1 + s_1)(\log m_1 + \log m_2)/n}$ established by [6] and $\sqrt{(m_1 + m_2)\log[\max(m_1, m_2, n)]/(nm_2)}$ established by [7]. In literature, [5] shows that there exists a local minimizer of the objective function whose estimation errors match ours. However, it is unknown if their estimator can achieve such convergence rate. On the other hand, our theorem confirms that our algorithm is able to find such estimator with optimal rate of convergence.

3.2 Estimation error in max norm and spectral norm

We next show the estimation error in max norm and spectral norm. Trivially, these estimation errors are bounded by that in Frobenius norm shown in Theorem 3.5. To develop improved rates of convergence in max and spectral norms, we need to impose stronger conditions on true parameters.

We first introduce some important notations. Denote d_k as the maximum number of non-zeros in any row of the true precision matrices $\mathbf{\Omega}_k^*$, that is,

$$d_k := \max_{i \in \{1,\dots,m_k\}} \left| \{ j \in \{1,\dots,m_k\} : [\mathbf{\Omega}_k^*]_{i,j} \neq 0 \} \right|, \tag{3.7}$$

with $|\cdot|$ the cardinality of the inside set. For each covariance matrix $\mathbf{\Sigma}_k^*$, we define $\kappa_{\mathbf{\Sigma}_k^*} := \|\|\mathbf{\Sigma}_k^*\|\|_\infty$. Denote the Hessian matrix $\mathbf{\Gamma}_k^* := \mathbf{\Omega}_k^{*-1} \otimes \mathbf{\Omega}_k^{*-1} \in \mathbb{R}^{m_k^2 \times m_k^2}$, whose entry $[\mathbf{\Gamma}_k^*]_{(i,j),(s,t)}$ corresponds to the second order partial derivative of the objective function with respect to $[\mathbf{\Omega}_k]_{i,j}$ and $[\mathbf{\Omega}_k]_{s,t}$. We define its sub-matrix indexed by the index set $\mathbb{S}_k$ as $[\mathbf{\Gamma}_k^*]_{\mathbb{S}_k,\mathbb{S}_k} = [\mathbf{\Omega}_k^{*-1} \otimes \mathbf{\Omega}_k^{*-1}]_{\mathbb{S}_k,\mathbb{S}_k}$, which is the $|\mathbb{S}_k| \times |\mathbb{S}_k|$ matrix with rows and columns of $\mathbf{\Gamma}_k^*$ indexed by $\mathbb{S}_k$ and $\mathbb{S}_k$, respectively. Moreover, we define $\kappa_{\mathbf{\Gamma}_k^*} := \|\|([\mathbf{\Gamma}_k^*]_{\mathbb{S}_k,\mathbb{S}_k})^{-1}\|\|_\infty$. In order to establish the rate of convergence in max norm, we need to impose an irrepresentability condition on the Hessian matrix.

Condition 3.7 (Irrepresentability). For each $k = 1,\dots,K$, there exists some $\alpha_k \in (0,1]$ such that

$$\max_{e \in \mathbb{S}_k^c} \left\| [\mathbf{\Gamma}_k^*]_{e,\mathbb{S}_k} \left([\mathbf{\Gamma}_k^*]_{\mathbb{S}_k,\mathbb{S}_k} \right)^{-1} \right\|_1 \leq 1 - \alpha_k.$$

Condition 3.7 controls the influence of the non-connected terms in $\mathbb{S}_k^c$ on the connected edges in $\mathbb{S}_k$. This condition has been widely applied in lasso penalized models [26, 27].

Condition 3.8 (Bounded Complexity). For each $k = 1,\dots,K$, the parameters $\kappa_{\mathbf{\Sigma}_k^*}, \kappa_{\mathbf{\Gamma}_k^*}$ are bounded and the parameter d_k in (3.7) satisfies $d_k = o\left(\sqrt{nm}/(m_k \log m_k)\right)$.

Theorem 3.9. Suppose Conditions 3.2, 3.3, 3.7 and 3.8 hold. Assume $s_k = O(m_k)$ for $k = 1,\dots,K$ and assume $m_k's$ are in the same order, i.e., $m_1 \asymp m_2 \asymp \cdots \asymp m_K$. For each k, if the initialization satisfies $\mathbf{\Omega}_j^{(0)} \in \mathbb{B}(\mathbf{\Omega}_j^*)$ for any $j \neq k$, then the estimator $\widehat{\mathbf{\Omega}}_k$ from Algorithm 1 with $T = 2$ satisfies,

$$\left\| \widehat{\mathbf{\Omega}}_k - \mathbf{\Omega}_k^* \right\|_\infty = O_P \left(\sqrt{\frac{m_k \log m_k}{nm}} \right). \tag{3.8}$$

In addition, the edge set of $\widehat{\mathbf{\Omega}}_k$ is a subset of the true edge set of $\mathbf{\Omega}_k^*$, that is, $\text{supp}(\widehat{\mathbf{\Omega}}_k) \subseteq \text{supp}(\mathbf{\Omega}_k^*)$.

Theorem 3.9 shows that our Tlasso estimator achieves the optimal rate of convergence in max norm [4]. Here we consider the estimator obtained after two iterations since we require a new concentration inequality (Lemma B.3) for the sample covariance matrix, which is built upon the estimator in Theorem 3.5. A direct consequence from Theorem 3.9 is the estimation error in spectral norm.

Corollary 3.10. Suppose the conditions of Theorem 3.9 hold, for any $k = 1,\dots,K$, we have

$$\left\| \widehat{\mathbf{\Omega}}_k - \mathbf{\Omega}_k^* \right\|_2 = O_P \left(d_k \sqrt{\frac{m_k \log m_k}{nm}} \right). \tag{3.9}$$

Remark 3.11. Now we compare our obtained rate of convergence in spectral norm for $K = 2$ with that established in the sparse matrix graphical model literature. In particular, [8] establishes the rate of $O_P\left(\sqrt{m_k(s_k \vee 1)\log(m_1 \vee m_2)/(nm_k)}\right)$ for $k = 1,2$. Therefore, when $d_k^2 \leq (s_k \vee 1)$, which holds for example in the bounded degree graphs, our obtained rate is faster. However, our faster rate comes at the price of assuming the irrepresentability condition. Using recent advance in nonconvex regularization [28], we can eliminate the irrepresentability condition. We leave this to future work.

3.3 Model selection consistency

Theorem 3.9 ensures that the estimated precision matrix correctly excludes all non-informative edges and includes all the true edges (i,j) with $|[\mathbf{\Omega}_k^*]_{i,j}| > C\sqrt{m_k \log m_k/(nm)}$ for some constant $C > 0$. Therefore, in order to achieve the model selection consistency, a sufficient condition is to assume that, for each $k = 1,\dots,K$, the minimal signal $\theta_k := \min_{(i,j) \in \text{supp}(\mathbf{\Omega}_k^*)} [\mathbf{\Omega}_k^*]_{i,j}$ is not too small.

Theorem 3.12. Under the conditions of Theorem 3.9, if $\theta_k \geq C\sqrt{m_k \log m_k/(nm)}$ for some constant $C > 0$, then for any $k = 1,\dots,K$, $\text{sign}(\widehat{\mathbf{\Omega}}_k) = \text{sign}(\mathbf{\Omega}_k^*)$, with high probability.

Theorem 3.12 indicates that our Tlasso estimator is able to correctly recover the graphical structure of each way of the high-dimensional tensor data. To the best of our knowledge, these is the first model selection consistency result in high dimensional tensor graphical model.

4 Simulations

We compare the proposed Tlasso estimator with two alternatives. The first one is the direct graphical lasso (Glasso) approach [21] which applies the glasso to the vectorized tensor data to estimate $\boldsymbol{\Omega}_1^* \otimes \cdots \otimes \boldsymbol{\Omega}_K^*$ directly. The second alternative method is the iterative penalized maximum likelihood method (P-MLE) proposed by [9], whose termination condition is set to be $\sum_{k=1}^K \|\widehat{\boldsymbol{\Omega}}_k^{(t)} - \widehat{\boldsymbol{\Omega}}_k^{(t-1)}\|_F / K \le 0.001$.

For simplicity, in our Tlasso algorithm we set the initialization of k-th precision matrix as $\mathbb{1}_{m_k}$ for each $k = 1, \ldots, K$ and the total iteration $T = 1$. The tuning parameter λ_k is set as $20\sqrt{\log m_k/(nmm_k)}$. For a fair comparison, the same tuning parameter is applied in the P-MLE method. In the direct Glasso approach, its tuning parameter is chosen by cross-validation via $huge$ package [29].

We consider two simulations with a third order tensor, i.e., $K = 3$. In Simulation 1, we construct a triangle graph, while in Simulation 2, we construct a four nearest neighbor graph for each precision matrix. An illustration of the generated graphs are shown in Figure 1. In each simulation, we consider three scenarios, i.e., s1: $n = 10$ and $(m_1, m_2, m_3) = (10, 10, 10)$; s2: $n = 50$ and $(m_1, m_2, m_3) = (10, 10, 10)$; s3: $n = 10$ and $(m_1, m_2, m_3) = (100, 5, 5)$. We repeat each example 100 times and compute the averaged computational time, the averaged estimation error of the Kronecker product of precision matrices $(m_1 m_2 m_3)^{-1}\|\widehat{\boldsymbol{\Omega}}_1 \otimes \cdots \otimes \widehat{\boldsymbol{\Omega}}_K - \boldsymbol{\Omega}_1^* \otimes \cdots \otimes \boldsymbol{\Omega}_K^*\|_F$, the true positive rate (TPR), and the true negative rate (TNR). More specifically, we denote $a_{i,j}^*$ be the (i, j)-th entry of $\boldsymbol{\Omega}_1^* \otimes \cdots \otimes \boldsymbol{\Omega}_K^*$, and define TPR $:= \sum_{i,j} \mathbb{1}(\widehat{a}_{i,j} \ne 0, a_{i,j}^* \ne 0)/\sum_{i,j} \mathbb{1}(a_{i,j}^* \ne 0)$ and TNR $:= \sum_{i,j} \mathbb{1}(\widehat{a}_{i,j} = 0, a_{i,j}^* = 0)/\sum_i \mathbb{1}(a_{i,j}^* = 0)$.

As shown in Figure 1, our Tlasso is dramatically faster than both alternative methods. In Scenario s3, Tlasso takes about five seconds for each replicate, the P-MLE takes about 500 seconds while the direct Glasso method takes more than one hour and is omitted in the plot. Tlasso algorithm is not only computationally efficient but also enjoys superior estimation accuracy. In all examples, the direct Glasso method has significantly larger errors than Tlasso due to ignoring the tensor graphical structure. Tlasso outperforms P-MLE in Scenarios s1 and s2 and is comparable to it in Scenario s3.
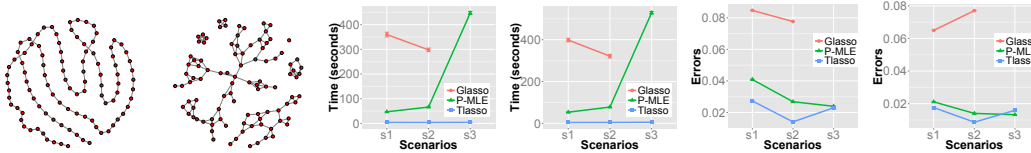

Figure 1: Left two plots: illustrations of the generated graphs; Middle two plots: computational time; Right two plots: estimation errors. In each group of two plots, the left (right) is for Simulation 1 (2).

Table 1 shows the variable selection performance. Our Tlasso identifies almost all edges in these six examples, while the Glasso and P-MLE method miss several true edges. On the other hand, Tlasso tends to include more non-connected edges than other methods.

Table 1: A comparison of variable selection performance. Here TPR and TNR denote the true positive rate and true negative rate.

Scenarios	Glasso		P-MLE		Tlasso	
	TPR	TNR	TPR	TNR	TPR	TNR
s1	0.27 (0.002)	0.96 (0.000)	1 (0)	0.89 (0.002)	1(0)	0.76 (0.004)
Sim 1 s2	0.34 (0.000)	0.93 (0.000)	1 (0)	0.89 (0.002)	1(0)	0.76 (0.004)
s3	/	/	1 (0)	0.93 (0.001)	1(0)	0.70 (0.004)
s1	0.08 (0.000)	0.96 (0.000)	0.93 (0.004)	0.88 (0.002)	1(0)	0.65 (0.005)
Sim 2 s2	0.15 (0.000)	0.92 (0.000)	1 (0)	0.85 (0.002)	1(0)	0.63 (0.005)
s3	/	/	0.82 (0.001)	0.93 (0.001)	0.99(0.001)	0.38 (0.002)

References

[1] S. Rendle and L. Schmidt-Thieme. Pairwise interaction tensor factorization for personalized tag recommendation. In *International Conference on Web Search and Data Mining*, 2010.

[2] G.I. Allen. Sparse higher-order principal components analysis. In *International Conference on Artificial Intelligence and Statistics*, 2012.

[3] J. Zahn, S. Poosala, A. Owen, D. Ingram, et al. AGEMAP: A gene expression database for aging in mice. *PLOS Genetics*, 3:2326–2337, 2007.

[4] T. Cai, W. Liu, and H.H. Zhou. Estimating sparse precision matrix: Optimal rates of convergence and adaptive estimation. *Annals of Statistics*, 2015.

[5] C. Leng and C.Y. Tang. Sparse matrix graphical models. *Journal of the American Statistical Association*, 107:1187–1200, 2012.

[6] J. Yin and H. Li. Model selection and estimation in the matrix normal graphical model. *Journal of Multivariate Analysis*, 107:119–140, 2012.

[7] T. Tsiligkaridis, A. O. Hero, and S. Zhou. On convergence of Kronecker graphical Lasso algorithms. *IEEE Transactions on Signal Processing*, 61:1743–1755, 2013.

[8] S. Zhou. Gemini: Graph estimation with matrix variate normal instances. *Annals of Statistics*, 42:532–562, 2014.

[9] S. He, J. Yin, H. Li, and X. Wang. Graphical model selection and estimation for high dimensional tensor data. *Journal of Multivariate Analysis*, 128:165–185, 2014.

[10] P. Jain, P. Netrapalli, and S. Sanghavi. Low-rank matrix completion using alternating minimization. In *Symposium on Theory of Computing*, pages 665–674, 2013.

[11] P. Netrapalli, P. Jain, and S. Sanghavi. Phase retrieval using alternating minimization. In *Advances in Neural Information Processing Systems*, pages 2796–2804, 2013.

[12] J. Sun, Q. Qu, and J. Wright. Complete dictionary recovery over the sphere. *arXiv:1504.06785*, 2015.

[13] S. Arora, R. Ge, T. Ma, and A. Moitra. Simple, efficient, and neural algorithms for sparse coding. *arXiv:1503.00778*, 2015.

[14] A. Anandkumar, R. Ge, D. Hsu, S. Kakade, and M. Telgarsky. Tensor decompositions for learning latent variable models. *Journal of Machine Learning Research*, 15:2773–2832, 2014.

[15] W. Sun, J. Lu, H. Liu, and G. Cheng. Provable sparse tensor decomposition. *arXiv:1502.01425*, 2015.

[16] S. Zhe, Z. Xu, X. Chu, Y. Qi, and Y. Park. Scalable nonparametric multiway data analysis. In *International Conference on Artificial Intelligence and Statistics*, 2015.

[17] S. Zhe, Z. Xu, Y. Qi, and P. Yu. Sparse bayesian multiview learning for simultaneous association discovery and diagnosis of alzheimer's disease. In *Twenty-Ninth AAAI Conference on Artificial Intelligence*, 2015.

[18] T. Kolda and B. Bader. Tensor decompositions and applications. *SIAM Review*, 51:455–500, 2009.

[19] R. Tibshirani. Regression shrinkage and selection via the Lasso. *Journal of the Royal Statistical Society, Series B*, 58:267–288, 1996.

[20] M. Yuan and Y. Lin. Model selection and estimation in the gaussian graphical model. *Biometrika*, 94:19–35, 2007.

[21] J. Friedman, H. Hastie, and R. Tibshirani. Sparse inverse covariance estimation with the graphical Lasso. *Biostatistics*, 9:432–441, 2008.

[22] A. J. Rothman, P. J. Bickel, E. Levina, and J. Zhu. Sparse permutation invariant covariance estimation. *Electronic Journal of Statistics*, 2:494–515, 2008.

[23] W. Sun, J. Wang, and Y. Fang. Consistent selection of tuning parameters via variable selection stability. *Journal of Machine Learning Research*, 14:3419–3440, 2013.

[24] M. Ledoux and M. Talagrand. *Probability in Banach Spaces: Isoperimetry and Processes*. Springer, 2011.

[25] J. Fan, Y. Feng, and Y. Wu. Network exploration via the adaptive Lasso and scad penalties. *Annals of Statistics*, 3:521–541, 2009.

[26] P. Zhao and B. Yu. On model selection consistency of Lasso. *Journal of Machine Learning Research*, 7:2541–2567, 2006.

[27] P. Ravikumar, M.J. Wainwright, G. Raskutti, and B. Yu. High-dimensional covariance estimation by minimizing ℓ_1-penalized log-determinant divergence. *Electronic Journal of Statistics*, 5:935–980, 2011.

[28] Z. Wang, H. Liu, and T. Zhang. Optimal computational and statistical rates of convergence for sparse nonconvex learning problems. *Annals of Statistics*, 42:2164–2201, 2014.

[29] T. Zhao, H. Liu, K. Roeder, J. Lafferty, and L. Wasserman. The huge package for high-dimensional undirected graph estimation in R. *Journal of Machine Learning Research*, 13:1059–1062, 2012.

[30] A. Gupta and D. Nagar. *Matrix variate distributions*. Chapman and Hall/CRC Press, 2000.

[31] P. Hoff. Separable covariance arrays via the Tucker product, with applications to multivariate relational data. *Bayesian Analysis*, 6:179–196, 2011.

[32] A.P. Dawid. Some matrix-variate distribution theory: Notational considerations and a bayesian application. *Biometrika*, 68:265–274, 1981.

[33] S. Negahban and M.J. Wainwright. Estimation of (near) low-rank matrices with noise and high-dimensional scaling. *Annals of Statistics*, 39:1069–1097, 2011.

Non-convex Statistical Optimization for Sparse Tensor Graphical Model (Supplementary Material)

In this supplementary note, we provide the proofs of our main theorems in §A, prove the key lemmas in §B, list the auxiliary lemmas in §C, and illustrate additional simulation results in §D.

A Proof of main theorems

Proof of Theorem 3.1: To ease the presentation, we show that Theorem 3.1 holds when $K = 3$. The proof can be easily generalized to the case with $K > 3$.

We first simplify the population log-likelihood function. Note that when $\mathcal{T} \sim \mathrm{TN}(\mathbf{0}; \boldsymbol{\Sigma}_1^*, \boldsymbol{\Sigma}_2^*, \boldsymbol{\Sigma}_3^*)$, Lemma 1 of [9] implies that $\mathrm{vec}(\mathcal{T}) \sim \mathrm{N}(\mathrm{vec}(\mathbf{0}); \boldsymbol{\Sigma}_3^* \otimes \boldsymbol{\Sigma}_2^* \otimes \boldsymbol{\Sigma}_1^*)$. Therefore,

$$\mathbb{E}\big\{\mathrm{tr}\big[\mathrm{vec}(\mathcal{T})\mathrm{vec}(\mathcal{T})^\top(\boldsymbol{\Omega}_3 \otimes \boldsymbol{\Omega}_2 \otimes \boldsymbol{\Omega}_1)\big]\big\} = \mathrm{tr}\big[(\boldsymbol{\Sigma}_3^* \otimes \boldsymbol{\Sigma}_2^* \otimes \boldsymbol{\Sigma}_1^*)(\boldsymbol{\Omega}_3 \otimes \boldsymbol{\Omega}_2 \otimes \boldsymbol{\Omega}_1)\big]$$
$$= \mathrm{tr}(\boldsymbol{\Sigma}_3^*\boldsymbol{\Omega}_3)\mathrm{tr}(\boldsymbol{\Sigma}_2^*\boldsymbol{\Omega}_2)\mathrm{tr}(\boldsymbol{\Sigma}_1^*\boldsymbol{\Omega}_1),$$

where the second equality is due to the properties of kronecker product that $(\mathbf{A} \otimes \mathbf{B})(\mathbf{C} \otimes \mathbf{D}) = (\mathbf{AC}) \otimes (\mathbf{BD})$ and $\mathrm{tr}(\mathbf{A} \otimes \mathbf{B}) = \mathrm{tr}(\mathbf{A})\mathrm{tr}(\mathbf{B})$. Therefore, the population log-likelihood function can be rewritten as

$$q(\boldsymbol{\Omega}_1, \boldsymbol{\Omega}_2, \boldsymbol{\Omega}_3) = \frac{\mathrm{tr}(\boldsymbol{\Sigma}_3^*\boldsymbol{\Omega}_3)\mathrm{tr}(\boldsymbol{\Sigma}_2^*\boldsymbol{\Omega}_2)\mathrm{tr}(\boldsymbol{\Sigma}_1^*\boldsymbol{\Omega}_1)}{m_1 m_2 m_3} - \frac{1}{m_1}\log|\boldsymbol{\Omega}_1| - \frac{1}{m_2}\log|\boldsymbol{\Omega}_2| - \frac{1}{m_3}\log|\boldsymbol{\Omega}_3|.$$

Taking derivative of $q(\boldsymbol{\Omega}_1, \boldsymbol{\Omega}_2, \boldsymbol{\Omega}_3)$ with respect to $\boldsymbol{\Omega}_1$ while fixing $\boldsymbol{\Omega}_2$ and $\boldsymbol{\Omega}_3$, we have

$$\nabla_1 q(\boldsymbol{\Omega}_1, \boldsymbol{\Omega}_2, \boldsymbol{\Omega}_3) = \frac{\mathrm{tr}(\boldsymbol{\Sigma}_3^*\boldsymbol{\Omega}_3)\mathrm{tr}(\boldsymbol{\Sigma}_2^*\boldsymbol{\Omega}_2)}{m_1 m_2 m_3}\boldsymbol{\Sigma}_1^* - \frac{1}{m_1}\boldsymbol{\Omega}_1^{-1}.$$

Setting it as zero leads to $\boldsymbol{\Omega}_1 = m_2 m_3[\mathrm{tr}(\boldsymbol{\Sigma}_3^*\boldsymbol{\Omega}_3)\mathrm{tr}(\boldsymbol{\Sigma}_2^*\boldsymbol{\Omega}_2)]^{-1}\boldsymbol{\Omega}_1^*$. This is indeed a minimizer of $q(\boldsymbol{\Omega}_1, \boldsymbol{\Omega}_2, \boldsymbol{\Omega}_3)$ when fixing $\boldsymbol{\Omega}_2$ and $\boldsymbol{\Omega}_3$, since the second derivative $\nabla_1^2 q(\boldsymbol{\Omega}_1, \boldsymbol{\Omega}_2, \boldsymbol{\Omega}_3) = m_1^{-1}\boldsymbol{\Omega}_1^{-1} \otimes \boldsymbol{\Omega}_1^{-1}$ is positive definite. Therefore, we have

$$M_1(\boldsymbol{\Omega}_2, \boldsymbol{\Omega}_3) = \frac{m_2 m_3}{\mathrm{tr}(\boldsymbol{\Sigma}_3^*\boldsymbol{\Omega}_3)\mathrm{tr}(\boldsymbol{\Sigma}_2^*\boldsymbol{\Omega}_2)}\boldsymbol{\Omega}_1^*. \tag{A.1}$$

Therefore, $M_1(\boldsymbol{\Omega}_2, \boldsymbol{\Omega}_3)$ equals to the true parameter $\boldsymbol{\Omega}_1^*$ up to a constant. The computations of $M_2(\boldsymbol{\Omega}_1, \boldsymbol{\Omega}_3)$ and $M_3(\boldsymbol{\Omega}_1, \boldsymbol{\Omega}_2)$ follow from the same argument. This ends the proof of Theorem 3.1. ∎

Proof of Theorem 3.4: To ease the presentation, we show that (3.5) holds when $K = 3$. The proof of the case when $K > 3$ is similar. We focus on the proof of the statistical error for the sample minimization function $\widehat{M_1}(\boldsymbol{\Omega}_2, \boldsymbol{\Omega}_3)$.

By definition, $\widehat{M_1}(\boldsymbol{\Omega}_2, \boldsymbol{\Omega}_3) = \mathrm{argmin}_{\boldsymbol{\Omega}_1} q_n(\boldsymbol{\Omega}_1, \boldsymbol{\Omega}_2, \boldsymbol{\Omega}_3) = \mathrm{argmin}_{\boldsymbol{\Omega}_1} L(\boldsymbol{\Omega}_1)$, where

$$L(\boldsymbol{\Omega}_1) = \frac{1}{m_1}\mathrm{tr}(\mathbf{S}_1\boldsymbol{\Omega}_1) - \frac{1}{m_1}\log|\boldsymbol{\Omega}_1| + \lambda_1\|\boldsymbol{\Omega}_1\|_{1,\mathrm{off}},$$

with the sample covariance matrix

$$\mathbf{S}_1 = \frac{1}{m_2 m_3 n}\sum_{i=1}^n \mathbf{V}_i\mathbf{V}_i^\top \text{ with } \mathbf{V}_i = \big[\mathcal{T}_i \times \{\mathbb{1}_{m_1}, \boldsymbol{\Omega}_2^{1/2}, \boldsymbol{\Omega}_3^{1/2}\}\big]_{(1)}.$$

For some constant $H > 0$, we define the set of convergence

$$\mathbb{A} := \left\{\boldsymbol{\Delta} \in \mathbb{R}^{m_1 \times m_1} : \boldsymbol{\Delta} = \boldsymbol{\Delta}^\top, \|\boldsymbol{\Delta}\|_F = H\sqrt{\frac{(m_1 + s_1)\log m_1}{nm_2 m_3}}\right\}.$$

The key idea is to show that

$$\inf_{\boldsymbol{\Delta} \in \mathbb{A}} \big\{L\big(M_1(\boldsymbol{\Omega}_2, \boldsymbol{\Omega}_3) + \boldsymbol{\Delta}\big) - L\big(M_1(\boldsymbol{\Omega}_2, \boldsymbol{\Omega}_3)\big)\big\} > 0, \tag{A.2}$$

with high probability. To understand it, note that the function $L\big(M_1(\boldsymbol{\Omega}_2, \boldsymbol{\Omega}_3) + \boldsymbol{\Delta}\big) - L\big(M_1(\boldsymbol{\Omega}_2, \boldsymbol{\Omega}_3)\big)$ is convex in $\boldsymbol{\Delta}$. In addition, since $\widehat{M}_1(\boldsymbol{\Omega}_2, \boldsymbol{\Omega}_3)$ minimizes $L(\boldsymbol{\Omega}_1)$, we have

$$L\big(\widehat{M}_1(\boldsymbol{\Omega}_2, \boldsymbol{\Omega}_3)\big) - L\big(M_1(\boldsymbol{\Omega}_2, \boldsymbol{\Omega}_3)\big) \leq L\big(M_1(\boldsymbol{\Omega}_2, \boldsymbol{\Omega}_3)\big) - L\big(M_1(\boldsymbol{\Omega}_2, \boldsymbol{\Omega}_3)\big) = 0.$$

If we can show (A.2), then the minimizer $\widehat{\boldsymbol{\Delta}} = \widehat{M}_1(\boldsymbol{\Omega}_2, \boldsymbol{\Omega}_3) - M_1(\boldsymbol{\Omega}_2, \boldsymbol{\Omega}_3)$ must be within the interior of the ball defined by $\mathbb{A}$, and hence $\|\widehat{\boldsymbol{\Delta}}\|_F \leq H\sqrt{(m_1 + s_1)\log m_1/(nm_2 m_3)}$. Similar technique is applied in vector-valued graphical model literature [25].

To show (A.2), we first decompose $L\big(M_1(\boldsymbol{\Omega}_2, \boldsymbol{\Omega}_3) + \boldsymbol{\Delta}\big) - L\big(M_1(\boldsymbol{\Omega}_2, \boldsymbol{\Omega}_3)\big) = I_1 + I_2 + I_3$, where

$$
\begin{aligned}
I_1 &:= \frac{1}{m_1}\mathrm{tr}(\boldsymbol{\Delta}\mathbf{S}_1) - \frac{1}{m_1}\big\{\log|M_1(\boldsymbol{\Omega}_2, \boldsymbol{\Omega}_3) + \boldsymbol{\Delta}| - \log|M_1(\boldsymbol{\Omega}_2, \boldsymbol{\Omega}_3)|\big\}, \\
I_2 &:= \lambda_1\big\{\|[M_1(\boldsymbol{\Omega}_2, \boldsymbol{\Omega}_3) + \boldsymbol{\Delta}]_{\mathbb{S}_1}\|_1 - \|[M_1(\boldsymbol{\Omega}_2, \boldsymbol{\Omega}_3)]_{\mathbb{S}_1}\|_1\big\}, \\
I_3 &:= \lambda_1\big\{\|[M_1(\boldsymbol{\Omega}_2, \boldsymbol{\Omega}_3) + \boldsymbol{\Delta}]_{\mathbb{S}_1^c}\|_1 - \|[M_1(\boldsymbol{\Omega}_2, \boldsymbol{\Omega}_3)]_{\mathbb{S}_1^c}\|_1\big\}.
\end{aligned}
$$

It is sufficient to show $I_1 + I_2 + I_3 > 0$ with high probability. To simplify the term I_1, we employ the Taylor expansion of $f(t) = \log|M_1(\boldsymbol{\Omega}_2, \boldsymbol{\Omega}_3) + t\boldsymbol{\Delta}|$ at $t = 0$ to obtain

$$
\begin{aligned}
&\log|M_1(\boldsymbol{\Omega}_2, \boldsymbol{\Omega}_3) + \boldsymbol{\Delta}| - \log|M_1(\boldsymbol{\Omega}_2, \boldsymbol{\Omega}_3)| \\
&= \mathrm{tr}\big\{[M_1(\boldsymbol{\Omega}_2, \boldsymbol{\Omega}_3)]^{-1}\boldsymbol{\Delta}\big\} - [\mathrm{vec}(\boldsymbol{\Delta})]^\top \left[\int_0^1 (1-\nu)\mathbf{M}_\nu^{-1} \otimes \mathbf{M}_\nu^{-1}\mathrm{d}\nu\right]\mathrm{vec}(\boldsymbol{\Delta}),
\end{aligned}
$$

where $\mathbf{M}_\nu := M_1(\boldsymbol{\Omega}_2, \boldsymbol{\Omega}_3) + \nu\boldsymbol{\Delta} \in \mathbb{R}^{m_1 \times m_1}$. This leads to

$$I_1 = \underbrace{\frac{1}{m_1}\mathrm{tr}\big(\{\mathbf{S}_1 - [M_1(\boldsymbol{\Omega}_2, \boldsymbol{\Omega}_3)]^{-1}\}\boldsymbol{\Delta}\big)}_{I_{11}} + \underbrace{\frac{1}{m_1}[\mathrm{vec}(\boldsymbol{\Delta})]^\top \left[\int_0^1 (1-\nu)\mathbf{M}_\nu^{-1} \otimes \mathbf{M}_\nu^{-1}\mathrm{d}\nu\right]\mathrm{vec}(\boldsymbol{\Delta})}_{I_{12}}.$$

For two symmetric matrices $\mathbf{A}, \mathbf{B}$, it is easy to see that $|\mathrm{tr}(\mathbf{A}\mathbf{B})| = |\sum_{i,j}\mathbf{A}_{i,j}\mathbf{B}_{i,j}|$. Based on this observation, we decompose I_{11} into two parts: those in the set $\mathbb{S}_1 = \{(i,j) : [\boldsymbol{\Omega}_1^*]_{i,j} \neq 0\}$ and those not in $\mathbb{S}_1$. That is, $|I_{11}| \leq I_{111} + I_{112}$, where

$$
\begin{aligned}
I_{111} &:= \frac{1}{m_1}\Big|\sum_{(i,j)\in\mathbb{S}_1}\big\{\mathbf{S}_1 - [M_1(\boldsymbol{\Omega}_2, \boldsymbol{\Omega}_3)]^{-1}\big\}_{i,j}\boldsymbol{\Delta}_{i,j}\Big|, \\
I_{112} &:= \frac{1}{m_1}\Big|\sum_{(i,j)\notin\mathbb{S}_1}\big\{\mathbf{S}_1 - [M_1(\boldsymbol{\Omega}_2, \boldsymbol{\Omega}_3)]^{-1}\big\}_{i,j}\boldsymbol{\Delta}_{i,j}\Big|.
\end{aligned}
$$

Bound I_{111}: For two matrices $\mathbf{A}, \mathbf{B}$ and a set $\mathbb{S}$, we have

$$\Big|\sum_{(i,j)\in\mathbb{S}}\mathbf{A}_{i,j}\mathbf{B}_{i,j}\Big| \leq \max_{i,j}|\mathbf{A}_{i,j}|\Big|\sum_{(i,j)\in\mathbb{S}}\mathbf{B}_{i,j}\Big| \leq \sqrt{|\mathbb{S}|}\max_{i,j}|\mathbf{A}_{i,j}|\|\mathbf{B}\|_F,$$

where the second inequality is due to the Cauchy-Schwarz inequality and the fact that $\sum_{(i,j)\in\mathbb{S}}\mathbf{B}_{i,j}^2 \leq \|\mathbf{B}\|_F^2$. Therefore, we have

$$
\begin{aligned}
I_{111} &\leq \frac{\sqrt{s_1 + m_1}}{m_1} \cdot \max_{i,j}\Big|\big\{\mathbf{S}_1 - [M_1(\boldsymbol{\Omega}_2, \boldsymbol{\Omega}_3)]^{-1}\big\}_{ij}\Big|\|\boldsymbol{\Delta}\|_F \\
&\leq C\sqrt{\frac{(m_1 + s_1)\log m_1}{nm_1^2 m_2 m_3}}\|\boldsymbol{\Delta}\|_F = \frac{CH \cdot (m_1 + s_1)\log m_1}{nm_1 m_2 m_3}, \quad\quad\quad \text{(A.3)}
\end{aligned}
$$

where (A.3) is from Lemma B.2, the definition of $M_1(\boldsymbol{\Omega}_2, \boldsymbol{\Omega}_3)$ in (A.1), and the fact that $\boldsymbol{\Delta} \in \mathbb{A}$.

Bound I_{12}: For any vector $\mathbf{v} \in \mathbb{R}^p$ and any matrix $\mathbf{A} \in \mathbb{R}^{p \times p}$, the variational form of Rayleigh quotients implies $\lambda_{\min}(\mathbf{A}) = \min_{\|\mathbf{x}\|=1}\mathbf{x}^\top\mathbf{A}\mathbf{x}$ and hence $\lambda_{\min}(\mathbf{A})\|\mathbf{v}\|^2 \leq \mathbf{v}^\top\mathbf{A}\mathbf{v}$. Setting $\mathbf{v} = \mathrm{vec}(\boldsymbol{\Delta})$ and $\mathbf{A} = \int_0^1 (1-\nu)\mathbf{M}_\nu^{-1} \otimes \mathbf{M}_\nu^{-1}\mathrm{d}\nu$ leads to

$$I_{12} \geq \frac{1}{m_1}\|\mathrm{vec}(\boldsymbol{\Delta})\|_2^2 \int_0^1 (1-\nu)\lambda_{\min}\big(\mathbf{M}_\nu^{-1} \otimes \mathbf{M}_\nu^{-1}\big)\mathrm{d}\nu.$$

Moreover, by the property of kronecker product, we have

$$\lambda_{\min}\left(\mathbf{M}_\nu^{-1} \otimes \mathbf{M}_\nu^{-1}\right) = [\lambda_{\min}(\mathbf{M}_\nu^{-1})]^2 = [\lambda_{\max}(\mathbf{M}_\nu)]^{-2}.$$

In addition, by definition, $\mathbf{M}_\nu = M_1(\boldsymbol{\Omega}_2, \boldsymbol{\Omega}_3) + \nu\boldsymbol{\Delta}$, and hence we have

$$\lambda_{\max}[M_1(\boldsymbol{\Omega}_2, \boldsymbol{\Omega}_3) + \nu\boldsymbol{\Delta}] \leq \lambda_{\max}[M_1(\boldsymbol{\Omega}_2, \boldsymbol{\Omega}_3)] + \lambda_{\max}(\nu\boldsymbol{\Delta}).$$

Therefore, we can bound I_{12} from below, that is,

$$
\begin{aligned}
I_{12} &\geq \frac{\|\text{vec}(\boldsymbol{\Delta})\|_2^2}{2m_1} \min_{0 \leq \nu \leq 1} \left[\lambda_{\max}[M_1(\boldsymbol{\Omega}_2, \boldsymbol{\Omega}_3)] + \lambda_{\max}(\nu\boldsymbol{\Delta})\right]^{-2} \\
&\geq \frac{\|\text{vec}(\boldsymbol{\Delta})\|_2^2}{2m_1} \left[\|M_1(\boldsymbol{\Omega}_2, \boldsymbol{\Omega}_3)\|_2 + \|\boldsymbol{\Delta}\|_2\right]^{-2}.
\end{aligned}
$$

On the boundary of $\mathbb{A}$, it holds that $\|\boldsymbol{\Delta}\|_2 \leq \|\boldsymbol{\Delta}\|_F = o(1)$. Moreover, according to (A.1), we have

$$\|M_1(\boldsymbol{\Omega}_2, \boldsymbol{\Omega}_3)\|_2 = \left|\frac{m_2 m_3}{\text{tr}(\boldsymbol{\Sigma}_3^*\boldsymbol{\Omega}_3)\text{tr}(\boldsymbol{\Sigma}_2^*\boldsymbol{\Omega}_2)}\right| \|\boldsymbol{\Omega}_1^*\|_2 \leq \frac{100}{81}\|\boldsymbol{\Sigma}_1^*\|_2 \leq \frac{1.5}{C_1}, \tag{A.4}$$

where the first inequality is due to

$$
\begin{aligned}
\text{tr}(\boldsymbol{\Sigma}_3^*\boldsymbol{\Omega}_3) &= \text{tr}[\boldsymbol{\Sigma}_3^*(\boldsymbol{\Omega}_3 - \boldsymbol{\Omega}_3^*) + \mathbb{1}_{m_3}] \geq m_3 - |\text{tr}[\boldsymbol{\Sigma}_3^*(\boldsymbol{\Omega}_3 - \boldsymbol{\Omega}_3^*)]| \\
&\geq m_3 - \|\boldsymbol{\Sigma}_3^*\|_F\|\boldsymbol{\Omega}_3 - \boldsymbol{\Omega}_3^*\|_F \geq m_3(1 - \alpha\|\boldsymbol{\Sigma}_3^*\|_2/\sqrt{m_3}) \geq 0.9m_3,
\end{aligned}
$$

for sufficiently large m_3. Similarly, it holds that $\text{tr}(\boldsymbol{\Sigma}_2^*\boldsymbol{\Omega}_2) \geq 0.9m_2$. The second inequality in (A.4) is due to Condition 3.2. This together with the fact that $\|\text{vec}(\boldsymbol{\Delta})\|_2 = \|\boldsymbol{\Delta}\|_F = o(1) \leq 0.5/C_1$ for sufficiently large n imply that

$$I_{12} \geq \frac{\|\text{vec}(\boldsymbol{\Delta})\|_2^2}{2m_1}\left(\frac{C_1}{2}\right)^2 = \frac{C_1^2 H^2}{8} \cdot \frac{(m_1 + s_1)\log m_1}{nm_1 m_2 m_3}, \tag{A.5}$$

which dominates the term I_{111} for sufficiently large H.

Bound I_2: To bound I_2, we apply the triangle inequality and then connect the ℓ_1 matrix norm with its Frobenius norm to obtain the final bound. Specifically, we have

$$|I_2| \leq \lambda_1 \|[\boldsymbol{\Delta}]_{\mathbb{S}_1}\|_1 = \lambda_1 \sum_{(i,j)\in\mathbb{S}_1} |\boldsymbol{\Delta}_{i,j}| \leq \lambda_1\sqrt{(s_1 + m_1)\sum_{(i,j)\in\mathbb{S}_1}\boldsymbol{\Delta}_{i,j}^2} \leq \lambda_1\sqrt{s_1 + m_1}\|\boldsymbol{\Delta}\|_F,$$

where the first inequality is from triangle inequality, the second inequality is due to the Cauchy-Schwarz inequality by noting that $s_1 = |\mathbb{S}_1| - m_1$, and the last inequality is due to the definition of Frobenius norm. By Condition 3.3, $\lambda_1 \leq C_2\sqrt{\log m_1/(nm_1^2 m_2 m_3)}$. Therefore,

$$|I_2| \leq C_2 H \cdot \frac{(m_1 + s_1)\log m_1}{nm_1 m_2 m_3},$$

which is dominated by I_{12} for sufficiently large H according to (A.5).

Bound $I_3 - |I_{112}|$: We show $I_3 - |I_{112}| > 0$. According to (A.1), we have that $M_1(\boldsymbol{\Omega}_2, \boldsymbol{\Omega}_3)$ equals $\boldsymbol{\Omega}_1^*$ up to a non-zero coefficient. Therefore, for any entry $(i, j) \in \mathbb{S}_1^c$, we have $[M_1(\boldsymbol{\Omega}_2, \boldsymbol{\Omega}_3)]_{i,j} = 0$. This implies that

$$I_3 = \lambda_1 \sum_{(i,j)\in\mathbb{S}_1^c}\left\{|[M_1(\boldsymbol{\Omega}_2, \boldsymbol{\Omega}_3)]_{i,j} + \boldsymbol{\Delta}_{i,j}| - |[M_1(\boldsymbol{\Omega}_2, \boldsymbol{\Omega}_3)]_{i,j}|\right\} = \lambda_1 \sum_{(i,j)\in\mathbb{S}_1^c}|\boldsymbol{\Delta}_{i,j}|.$$

This together with the expression of I_{112} and the bound in Lemma B.2 leads to

$$
\begin{aligned}
I_3 - I_{112} &= \sum_{(i,j)\in\mathbb{S}_1^c}\left\{\lambda_1 - m_1^{-1}\left\{\mathbf{S}_1 - [M_1(\boldsymbol{\Omega}_2, \boldsymbol{\Omega}_3)]^{-1}\right\}_{i,j}\right\}|\boldsymbol{\Delta}_{i,j}| \\
&\geq \left(\lambda_1 - C\sqrt{\frac{\log m_1}{nm_1^2 m_2 m_3}}\right)\sum_{(i,j)\in\mathbb{S}_1^c}|\boldsymbol{\Delta}_{i,j}| > 0,
\end{aligned}
$$

3

as long as $1/C_2 > C$ for some constant C, which is valid for sufficient small C_2 in Condition 3.3.

Combining all these bounds together, we have, for any $\boldsymbol{\Delta} \in \mathbb{A}$, with high probability,

$$L\big(M_1(\boldsymbol{\Omega}_2, \boldsymbol{\Omega}_3) + \boldsymbol{\Delta}\big) - L\big(M_1(\boldsymbol{\Omega}_2, \boldsymbol{\Omega}_3)\big) \geq I_{12} - I_{111} - |I_2| + I_3 - I_{112} > 0,$$

which ends the proof Theorem 3.4. ∎

Proof of Theorem 3.5: We show it by connecting the one-step convergence result in Theorem 3.1 and the statistical error result in Theorem 3.4. We show the case when $K = 3$. The proof of the $K > 3$ case is similar. We focus on the proof of the estimation error $\big\|\widehat{\boldsymbol{\Omega}}_1 - \boldsymbol{\Omega}_1^*\big\|_F$.

To ease the presentation, in the following derivation we remove the superscript in the initializations $\boldsymbol{\Omega}_2^{(0)}$ and $\boldsymbol{\Omega}_3^{(0)}$ and use $\boldsymbol{\Omega}_2$ and $\boldsymbol{\Omega}_3$ instead. According to the procedure in Algorithm 1, we have

$$
\begin{aligned}
\big\|\widehat{\boldsymbol{\Omega}}_1 - \boldsymbol{\Omega}_1^*\big\|_F &= \left\| \frac{\widehat{M}_1(\boldsymbol{\Omega}_2, \boldsymbol{\Omega}_3)}{\big\|\widehat{M}_1(\boldsymbol{\Omega}_2, \boldsymbol{\Omega}_3)\big\|_F} - \frac{\widehat{M}_1(\boldsymbol{\Omega}_2, \boldsymbol{\Omega}_3)}{\big\|\widehat{M}_1(\boldsymbol{\Omega}_2, \boldsymbol{\Omega}_3)\big\|_F} \right\|_F \\
&\leq \left\| \frac{\widehat{M}_1(\boldsymbol{\Omega}_2, \boldsymbol{\Omega}_3)}{\big\|\widehat{M}_1(\boldsymbol{\Omega}_2, \boldsymbol{\Omega}_3)\big\|_F} - \frac{M_1(\boldsymbol{\Omega}_2, \boldsymbol{\Omega}_3)}{\big\|\widehat{M}_1(\boldsymbol{\Omega}_2, \boldsymbol{\Omega}_3)\big\|_F} \right\|_F + \left\| \frac{M_1(\boldsymbol{\Omega}_2, \boldsymbol{\Omega}_3)}{\big\|\widehat{M}_1(\boldsymbol{\Omega}_2, \boldsymbol{\Omega}_3)\big\|_F} - \frac{M_1(\boldsymbol{\Omega}_2, \boldsymbol{\Omega}_3)}{\big\|M_1(\boldsymbol{\Omega}_2, \boldsymbol{\Omega}_3)\big\|_F} \right\|_F \\
&\leq \frac{2}{\big\|\widehat{M}_1(\boldsymbol{\Omega}_2, \boldsymbol{\Omega}_3)\big\|_F} \big\|\widehat{M}_1(\boldsymbol{\Omega}_2, \boldsymbol{\Omega}_3) - M_1(\boldsymbol{\Omega}_2, \boldsymbol{\Omega}_3)\big\|_F,
\end{aligned}
$$

where the last inequality is due to the triangle inequality $\big||a| - |b|\big| \leq |a - b|$ and the summation of two parts. We next bound $\big\|\widehat{M}_1(\boldsymbol{\Omega}_2, \boldsymbol{\Omega}_3)\big\|_F$. By triangle inequality,

$$\big\|\widehat{M}_1(\boldsymbol{\Omega}_2, \boldsymbol{\Omega}_3)\big\|_F \geq \|M_1(\boldsymbol{\Omega}_2, \boldsymbol{\Omega}_3)\|_F - \big\|M_1(\boldsymbol{\Omega}_2, \boldsymbol{\Omega}_3) - \widehat{M}_1(\boldsymbol{\Omega}_2, \boldsymbol{\Omega}_3)\big\|_F \geq 2^{-1}\|M_1(\boldsymbol{\Omega}_2, \boldsymbol{\Omega}_3)\|_F,$$

since $\big\|M_1(\boldsymbol{\Omega}_2, \boldsymbol{\Omega}_3) - \widehat{M}_1(\boldsymbol{\Omega}_2, \boldsymbol{\Omega}_3)\big\|_F = o_P(1)$ as shown in Theorem 3.4. Moreover, by the Cauchy-Schwarz inequality, we have

$$\mathrm{tr}(\boldsymbol{\Sigma}_2^* \boldsymbol{\Omega}_2) \leq \|\boldsymbol{\Sigma}_2^*\|_F \|\boldsymbol{\Omega}_2\|_F \leq m_2 \|\boldsymbol{\Sigma}_2^*\|_2 \|\boldsymbol{\Omega}_2\|_2 \leq 2m_2/C_1,$$

due to Condition 3.2 and the fact that $\boldsymbol{\Omega}_2 \in \mathbb{B}(\boldsymbol{\Omega}_2^*)$. Similarly, we have $\mathrm{tr}(\boldsymbol{\Sigma}_3^* \boldsymbol{\Omega}_3) \leq 2m_3/C_1$. This together with the expression of $M_1(\boldsymbol{\Omega}_2, \boldsymbol{\Omega}_3)$ in (A.1) imply that $\big\|\widehat{M}_1(\boldsymbol{\Omega}_2, \boldsymbol{\Omega}_3)\big\|_F \geq C_1^2/4$ and hence

$$\big\|\widehat{\boldsymbol{\Omega}}_1 - \boldsymbol{\Omega}_1^*\big\|_F \leq \frac{8}{C_1^2} \big\|\widehat{M}_1(\boldsymbol{\Omega}_2, \boldsymbol{\Omega}_3) - M_1(\boldsymbol{\Omega}_2, \boldsymbol{\Omega}_3)\big\|_F = O_P\left(\sqrt{\frac{m_1(m_1 + s_1)\log m_1}{nm_1m_2m_3}} \right),$$

according to Theorem 3.4. This ends the proof Theorem 3.5. ∎

Proof of Theorem 3.9: We prove it by transferring the optimization problem to an equivalent primal-dual problem and then applying the convergence results of [27] to obtain the desirable rate of convergence.

Given the sample covariance matrix $\widehat{\mathbf{S}}_k$ defined in Lemma B.3, according to (2.3), for each $k = 1, \ldots, K$, the optimization problem has a unique solution $\widehat{\boldsymbol{\Omega}}_k$ which satisfies the following Karush-Kuhn-Tucker (KKT) conditions

$$\widehat{\mathbf{S}}_k - \widehat{\boldsymbol{\Omega}}_k + m_k \lambda_k \widehat{\mathbf{Z}}_k = 0, \tag{A.6}$$

where $\widehat{\mathbf{Z}}_k \in \mathbb{R}^{m_k \times m_k}$ belongs to the sub-differential of $\|\boldsymbol{\Omega}_k\|_{1,\mathrm{off}}$ evaluated at $\widehat{\boldsymbol{\Omega}}_k$, that is,

$$
[\widehat{\mathbf{Z}}_k]_{i,j} := \begin{cases} 0, & \text{if } i = j \\ \mathrm{sign}([\widehat{\boldsymbol{\Omega}}_k]_{i,j}) & \text{if } i \neq j \text{ and } [\widehat{\boldsymbol{\Omega}}_k]_{i,j} \neq 0 \\ \in [-1, +1] & \text{if } i \neq j \text{ and } [\widehat{\boldsymbol{\Omega}}_k]_{i,j} = 0. \end{cases}
$$

Following [27], we construct the primary-dual witness solution $(\widetilde{\boldsymbol{\Omega}}_k, \widetilde{\mathbf{Z}}_k)$ such that

$$\widetilde{\boldsymbol{\Omega}}_k := \underset{\boldsymbol{\Omega}_k \succ 0, \boldsymbol{\Omega}_k = \boldsymbol{\Omega}_k^\top, [\boldsymbol{\Omega}_k]_{\mathbb{S}_k^c} = 0}{\mathrm{argmin}} \left\{ \mathrm{tr}(\widehat{\mathbf{S}}_k \boldsymbol{\Omega}_k) - \log|\boldsymbol{\Omega}_k| + m_k \lambda_k \|\boldsymbol{\Omega}_k\|_{1,\mathrm{off}} \right\},$$

where the set $\mathbb{S}_k$ refers to the set of true non-zero edges of $\mathbf{\Omega}_k^*$. Therefore, by construction, the support of the dual estimator $\widetilde{\mathbf{\Omega}}_k$ is a subset of the true support, i.e., $\mathrm{supp}(\widetilde{\mathbf{\Omega}}_k) \subseteq \mathrm{supp}(\mathbf{\Omega}_k^*)$. We then construct $\widetilde{\mathbf{Z}}_k$ as the sub-differential $\widehat{\mathbf{Z}}_k$ and then for each $(i,j) \in \mathbb{S}_k^c$, we replace $[\widetilde{\mathbf{Z}}_k]_{i,j}$ with $([\widetilde{\mathbf{\Omega}}_k^{-1}]_{i,j} - [\widehat{\mathbf{S}}_k]_{i,j})/(m_k \lambda_k)$ to ensure that $(\widetilde{\mathbf{\Omega}}_k, \widetilde{\mathbf{Z}}_k)$ satisfies the optimality condition (A.6).

Denote $\mathbf{\Delta} := \widetilde{\mathbf{\Omega}}_k - \mathbf{\Omega}_k^*$ and $R(\mathbf{\Delta}) := \widetilde{\mathbf{\Omega}}_k^{-1} - \mathbf{\Omega}_k^{*-1} + \mathbf{\Omega}_k^{*-1} \mathbf{\Delta} \widetilde{\mathbf{\Omega}}_k^{-1}$. According to Lemma 4 of [27], in order to show the strict dual feasibility $\widetilde{\mathbf{\Omega}}_k = \widehat{\mathbf{\Omega}}_k$, it is sufficient to prove

$$\max\{\|\widehat{\mathbf{S}}_k - \mathbf{\Sigma}_k^*\|_\infty, \|R(\mathbf{\Delta})\|_\infty\} \leq \frac{\alpha_k m_k \lambda_k}{8},$$

with α_k defined in Condition 3.7. As assumed in Condition 3.3, the tuning parameter satisfies $1/C_2 \sqrt{\log m_k/(nmm_k)} \leq \lambda_k \leq C_2 \sqrt{\log m_k/(nmm_k)}$ for some constant $C_2 > 0$ and hence $\alpha_k m_k \lambda_k/8 \geq C_3 \sqrt{m_k \log m_k/(nm)}$ for some constant $C_3 > 0$.

In addition, according to Lemma B.3, we have

$$\|\widehat{\mathbf{S}}_k - \mathbf{\Sigma}_k^*\|_\infty = O_P\left(\max_{j=1,\ldots,K} \sqrt{\frac{(m_j + s_j)\log m_j}{nm}}\right).$$

Under the assumption that $s_j = O(m_j)$ for $j = 1, \ldots, K$ and $m_1 \asymp m_2 \asymp \cdots \asymp m_K$, we have

$$\|\widehat{\mathbf{S}}_k - \mathbf{\Sigma}_k^*\|_\infty = O_P\left(\sqrt{\frac{m_k \log m_k}{nm}}\right).$$

Therefore, there exists a sufficiently small constant C_2 such that $\|\widehat{\mathbf{S}}_k - \mathbf{\Sigma}_k^*\|_\infty \leq \alpha_k m_k \lambda_k/8$.

Moreover, according to Lemma 5 of [27], $\|R(\mathbf{\Delta})\|_\infty \leq 1.5 d_k \|\mathbf{\Delta}\|_\infty^2 \kappa_{\mathbf{\Sigma}_k^*}^3$ as long as $\|\mathbf{\Delta}\|_\infty \leq (3\kappa_{\mathbf{\Sigma}_k^*} d_k)^{-1}$. According to Lemma 6 of [27], if we can show

$$r := 2\kappa_{\mathbf{\Gamma}_k^*}\left(\|\widehat{\mathbf{S}}_k - \mathbf{\Sigma}_k^*\|_\infty + m_k \lambda_k\right) \leq \min\left\{\frac{1}{3\kappa_{\mathbf{\Sigma}_k^*} d_k}, \frac{1}{\kappa_{\mathbf{\Sigma}_k^*}^3 \kappa_{\mathbf{\Gamma}_k^*} d_k}\right\},$$

then we have $\|\mathbf{\Delta}\|_\infty \leq r$. By Condition 3.8, $\kappa_{\mathbf{\Gamma}_k^*}$ and $\kappa_{\mathbf{\Sigma}_k^*}$ are bounded. Therefore, $\|\widehat{\mathbf{S}}_k - \mathbf{\Sigma}_k^*\|_\infty + m_k \lambda_k$ is in the same order of $\sqrt{m_k \log m_k/(nm)}$, which is in a smaller order of d_k^{-1} by the assumption of d_k in Condition 3.8. Therefore, we have shown that $\|R(\mathbf{\Delta})\|_\infty \leq m_k \lambda_k$ for a sufficiently small constant C_2.

Combining above two bounds, we achieve the strict dual feasibility $\widetilde{\mathbf{\Omega}}_k = \widehat{\mathbf{\Omega}}_k$. Therefore, we have $\mathrm{supp}(\widehat{\mathbf{\Omega}}_k) \subseteq \mathrm{supp}(\mathbf{\Omega}_k^*)$ and moreover,

$$\|\widehat{\mathbf{\Omega}}_k - \mathbf{\Omega}_k^*\|_\infty = \|\mathbf{\Delta}\|_\infty = O_P\left(\sqrt{\frac{m_k \log m_k}{nm}}\right).$$

This ends the proof of Theorem 3.9. ∎

B Proof of key lemmas

The first key lemma establishes the rate of convergence of the difference between a sample-based quadratic form and its expectation. This new concentration result is also of independent interest.

Lemma B.1. Assume i.i.d. data $\mathbf{X}, \mathbf{X}_1, \ldots, \mathbf{X}_n \in \mathbb{R}^{p \times q}$ follows the matrix-variate normal distribution such that $\mathrm{vec}(\mathbf{X}_i) \sim N(\mathbf{0}; \mathbf{\Psi}^* \otimes \mathbf{\Sigma}^*)$ with $\mathbf{\Psi}^* \in \mathbb{R}^{q \times q}$ and $\mathbf{\Sigma}^* \in \mathbb{R}^{p \times p}$. Assume that $0 < C_1 \leq \lambda_{\min}(\mathbf{\Sigma}^*) \leq \lambda_{\max}(\mathbf{\Sigma}^*) \leq 1/C_1 < \infty$ and $0 < C_2 \leq \lambda_{\min}(\mathbf{\Psi}^*) \leq \lambda_{\max}(\mathbf{\Psi}^*) \leq 1/C_2 < \infty$ for some positive constants C_1, C_2. For any symmetric and positive definite matrix $\mathbf{\Omega} \in \mathbb{R}^{p \times p}$, we have

$$\max_{i,j}\left\{\frac{1}{np}\sum_{i=1}^n \mathbf{X}_i^\top \mathbf{\Omega} \mathbf{X}_i - \frac{1}{p}\mathbb{E}(\mathbf{X}^\top \mathbf{\Omega} \mathbf{X})\right\}_{i,j} = O_P\left(\sqrt{\frac{\log q}{np}}\right).$$

Proof of Lemma B.1: Consider a random matrix $\mathbf{X}$ following the matrix normal distribution such that $\text{vec}(\mathbf{X}) \sim \text{N}(\mathbf{0}; \boldsymbol{\Psi}^* \otimes \boldsymbol{\Sigma}^*)$. Let $\boldsymbol{\Lambda}^* = \boldsymbol{\Psi}^{*-1}$ and $\boldsymbol{\Omega}^* = \boldsymbol{\Sigma}^{*-1}$. Let $\mathbf{Y} := (\boldsymbol{\Omega}^*)^{1/2} \mathbf{X} (\boldsymbol{\Lambda}^*)^{1/2}$. According to the properties of matrix normal distribution [30], $\mathbf{Y}$ follows a matrix normal distribution such that $\text{vec}(\mathbf{Y}) \sim \text{N}(\mathbf{0}; \mathbb{1}_q \otimes \mathbb{1}_p)$, that is, all the entries of $\mathbf{Y}$ are i.i.d. standard Gaussian random variables. Next we rewrite the term $\mathbf{X}^\top \boldsymbol{\Omega} \mathbf{X}$ by $\mathbf{Y}$ and then simplify it. Simple algebra implies that

$$\mathbf{X}^\top \boldsymbol{\Omega} \mathbf{X} = (\boldsymbol{\Lambda}^*)^{-1/2} \mathbf{Y}^\top (\boldsymbol{\Omega}^*)^{-1/2} \boldsymbol{\Omega} (\boldsymbol{\Omega}^*)^{-1/2} \mathbf{Y} (\boldsymbol{\Lambda}^*)^{-1/2}.$$

When $\boldsymbol{\Omega}$ is symmetric and positive definite, the matrix $\mathbf{M} := (\boldsymbol{\Omega}^*)^{-1/2} \boldsymbol{\Omega} (\boldsymbol{\Omega}^*)^{-1/2} \in \mathbb{R}^{p \times p}$ is also symmetric and positive definite with Cholesky decomposition $\mathbf{U}^\top \mathbf{U}$, where $\mathbf{U} \in \mathbb{R}^{p \times p}$. Therefore,

$$\mathbf{X}^\top \boldsymbol{\Omega} \mathbf{X} = (\boldsymbol{\Lambda}^*)^{-1/2} \mathbf{Y}^\top \mathbf{U}^\top \mathbf{U} \mathbf{Y} (\boldsymbol{\Lambda}^*)^{-1/2}.$$

Moreover, denote the column of the matrix $(\boldsymbol{\Lambda}^*)^{-1/2}$ as $(\boldsymbol{\Lambda}^*)_{(j)}^{-1/2}$ and denote its row as $(\boldsymbol{\Lambda}^*)_i^{-1/2}$ for $i, j = 1, \ldots, q$. Define the standard basis $\mathbf{e}_i \in \mathbb{R}^q$ as the vector with 1 in its i-th entry and 0 in all the rest entries. The (s, t)-th entry of matrix $\mathbf{X}^\top \boldsymbol{\Omega} \mathbf{X}$ can be written as

$$\left\{ \mathbf{X}^\top \boldsymbol{\Omega} \mathbf{X} \right\}_{s,t} = \mathbf{e}_s^\top \mathbf{X}^\top \boldsymbol{\Omega} \mathbf{X} \mathbf{e}_t = (\boldsymbol{\Lambda}^*)_s^{-1/2} \mathbf{Y}^\top \mathbf{U}^\top \mathbf{U} \mathbf{Y} (\boldsymbol{\Lambda}^*)_{(t)}^{-1/2}.$$

For the sample matrices $\mathbf{X}_1, \ldots, \mathbf{X}_n$, we apply similar transformation that $\mathbf{Y}_i = (\boldsymbol{\Omega}^*)^{1/2} \mathbf{X}_i (\boldsymbol{\Lambda}^*)^{1/2}$. We apply the above derivation to the sample-based quadratic term $\mathbf{X}_i^\top \boldsymbol{\Omega} \mathbf{X}_i$. Let $\mathbf{A} = (\mathbf{a}_1, \ldots, \mathbf{a}_n) \in \mathbb{R}^{p \times n}$ with $\mathbf{a}_i = \mathbf{U} \mathbf{Y}_i (\boldsymbol{\Lambda}^*)_s^{-1/2} \in \mathbb{R}^p$ and $\mathbf{B} = (\mathbf{b}_1, \ldots, \mathbf{b}_n) \in \mathbb{R}^{p \times n}$ with $\mathbf{b}_i = \mathbf{U} \mathbf{Y}_i (\boldsymbol{\Lambda}^*)_t^{-1/2} \in \mathbb{R}^p$. Then we have

$$
\begin{aligned}
\left\{ \frac{1}{np} \sum_{i=1}^n \mathbf{X}_i^\top \boldsymbol{\Omega} \mathbf{X}_i \right\}_{s,t} &= \frac{1}{np} \sum_{i=1}^n \mathbf{a}_i^\top \mathbf{b}_i = \frac{1}{np} \sum_{i=1}^n \sum_{j=1}^p \mathbf{A}_{i,j} \mathbf{B}_{i,j} \\
&= \frac{1}{4np} \sum_{i=1}^n \sum_{j=1}^p \left\{ (\mathbf{A}_{i,j} + \mathbf{B}_{i,j})^2 - (\mathbf{A}_{i,j} - \mathbf{B}_{i,j})^2 \right\} \\
&= \frac{1}{4np} \left\{ \| \text{vec}(\mathbf{A}) + \text{vec}(\mathbf{B}) \|_2^2 + \| \text{vec}(\mathbf{A}) - \text{vec}(\mathbf{B}) \|_2^2 \right\}. \quad \text{(B.1)}
\end{aligned}
$$

Next we derive the explicit form of $\text{vec}(\mathbf{A})$ and $\text{vec}(\mathbf{B})$ in (B.1). Remind that $(\boldsymbol{\Lambda}^*)_s^{-1/2}$ is a vector of length q. By the property of matrix products, we can rewrite $\mathbf{a}_i = [(\boldsymbol{\Lambda}^*)_s^{-1/2} \otimes \mathbf{U}] \text{vec}(\mathbf{Y}_i)$, where $\otimes$ is the Kronecker product. Therefore, we have

$$
\begin{aligned}
\text{vec}(\mathbf{A}) &= \left[\mathbb{1}_n \otimes (\boldsymbol{\Lambda}^*)_s^{-1/2} \otimes \mathbf{U} \right] \mathbf{t} := \mathbf{Q}_1 \mathbf{t}, \\
\text{vec}(\mathbf{B}) &= \left[\mathbb{1}_n \otimes (\boldsymbol{\Lambda}^*)_t^{-1/2} \otimes \mathbf{U} \right] \mathbf{t} := \mathbf{Q}_2 \mathbf{t},
\end{aligned}
$$

where $\mathbf{t} = \left\{ [\text{vec}(\mathbf{Y}_1)]^\top, \ldots, [\text{vec}(\mathbf{Y}_n)]^\top \right\}^\top \in \mathbb{R}^{npq}$ is a vector with npq i.i.d. standard normal entries. Here $\mathbf{Q}_1 := \mathbb{1}_n \otimes (\boldsymbol{\Lambda}^*)_s^{-1/2} \otimes \mathbf{U}$ and $\mathbf{Q}_2 := \mathbb{1}_n \otimes (\boldsymbol{\Lambda}^*)_t^{-1/2} \otimes \mathbf{U}$ with $\mathbf{Q}_1, \mathbf{Q}_2 \in \mathbb{R}^{np \times npq}$. By the property of multivariate normal distribution, we have

$$
\begin{aligned}
\text{vec}(\mathbf{A}) + \text{vec}(\mathbf{B}) &\sim \text{N}\big(0; (\mathbf{Q}_1 + \mathbf{Q}_2)(\mathbf{Q}_1 + \mathbf{Q}_2)^\top\big) := \text{N}(0; \mathbf{H}_1), \\
\text{vec}(\mathbf{A}) - \text{vec}(\mathbf{B}) &\sim \text{N}\big(0; (\mathbf{Q}_1 - \mathbf{Q}_2)(\mathbf{Q}_1 - \mathbf{Q}_2)^\top\big) := \text{N}(0; \mathbf{H}_2).
\end{aligned}
$$

Next, we bound the spectral norm of two matrices $\mathbf{H}_1$ and $\mathbf{H}_2$. By the property of matrix norm and the fact that one matrix and its transpose matrix have the same spectral norm, we have

$$\| \mathbf{H}_1 \|_2 \leq \| \mathbf{Q}_1 \mathbf{Q}_1^\top \|_2 + 2 \| \mathbf{Q}_1 \mathbf{Q}_2^\top \|_2 + \| \mathbf{Q}_2 \mathbf{Q}_2^\top \|_2,$$

then we bound each of these three terms individually. According to the definition of $\mathbf{Q}_1$ and the property of matrix Kronecker products, we have

$$
\begin{aligned}
\mathbf{Q}_1 \mathbf{Q}_1^\top &= \left[\mathbb{1}_n \otimes (\boldsymbol{\Lambda}^*)_s^{-1/2} \otimes \mathbf{U} \right] \left[\mathbb{1}_n \otimes (\boldsymbol{\Lambda}^*)_s^{-1/2} \otimes \mathbf{U} \right]^\top \\
&= \mathbb{1}_n \otimes (\boldsymbol{\Lambda}^*)_s^{-1/2} [(\boldsymbol{\Lambda}^*)_s^{-1/2}]^\top \otimes \mathbf{M},
\end{aligned}
$$

where the last equality is due to the fact that $(\mathbf{C}_1 \otimes \mathbf{C}_2)^\top = \mathbf{C}_1^\top \otimes \mathbf{C}_2^\top$ and $(\mathbf{C}_1 \otimes \mathbf{C}_2)(\mathbf{C}_3 \otimes \mathbf{C}_4) = (\mathbf{C}_1 \mathbf{C}_3) \otimes (\mathbf{C}_2 \mathbf{C}_4)$ for any matrices $\mathbf{C}_1, \ldots, \mathbf{C}_4$ such that the matrix multiplications $\mathbf{C}_1 \mathbf{C}_3$ and

6

$\mathbf{C}_2\mathbf{C}_4$ are valid. Moreover, we also use the Cholesky decomposition of $\mathbf{M}$, i.e., $\mathbf{M} = \mathbf{U}^\top\mathbf{U}$. Remind that $(\boldsymbol{\Lambda}^*)_s^{-1/2}[(\boldsymbol{\Lambda}^*)_s^{-1/2}]^\top \in \mathbb{R}$, therefore, the spectral norm $\mathbf{Q}_1\mathbf{Q}_1^\top$ can be written as

$$
\begin{aligned}
\|\mathbf{Q}_1\mathbf{Q}_1^\top\|_2 &= \left|(\boldsymbol{\Lambda}^*)_s^{-1/2}[(\boldsymbol{\Lambda}^*)_s^{-1/2}]^\top\right| \cdot \|\mathbb{1}_n\|_2\|\mathbf{M}\|_2 \\
&\leq \|\boldsymbol{\Psi}^*\|_2\|\mathbf{M}\|_2 \leq (1+\alpha/C_1)/C_2.
\end{aligned}
$$

Here the first inequality is because $\|\mathbb{1}_n\|_2 = 1$ and

$$
\begin{aligned}
\left|(\boldsymbol{\Lambda}^*)_s^{-1/2}[(\boldsymbol{\Lambda}^*)_s^{-1/2}]^\top\right| &= \left\|[(\boldsymbol{\Lambda}^*)_s^{-1/2}]^\top(\boldsymbol{\Lambda}^*)_s^{-1/2}\right\|_2 \leq \max_j \left\|[(\boldsymbol{\Psi}^*)_j^{1/2}]^\top(\boldsymbol{\Psi}^*)_j^{1/2}\right\|_2 \\
&\leq \left\|\sum_{j=1}^q [(\boldsymbol{\Psi}^*)_j^{1/2}]^\top(\boldsymbol{\Psi}^*)_j^{1/2}\right\|_2 = \|\boldsymbol{\Psi}^*\|_2,
\end{aligned}
$$

and the second inequality is because $\|\boldsymbol{\Psi}^*\|_2 \leq 1/C_2$ and

$$
\begin{aligned}
\|\mathbf{M}\|_2 &= \left\|(\boldsymbol{\Omega}^*)^{-1/2}\boldsymbol{\Omega}(\boldsymbol{\Omega}^*)^{-1/2}\right\|_2 = \|(\boldsymbol{\Omega}^*)^{-1/2}(\boldsymbol{\Omega}-\boldsymbol{\Omega}^*)(\boldsymbol{\Omega}^*)^{-1/2} + \mathbb{1}_p\|_2 \\
&\leq \|(\boldsymbol{\Omega}^*)^{-1/2}\|_2^2\|\boldsymbol{\Omega}-\boldsymbol{\Omega}^*\|_2 + 1 \leq \|\boldsymbol{\Sigma}^*\|_2\|\boldsymbol{\Omega}-\boldsymbol{\Omega}^*\|_F + 1 \leq 1 + \alpha/C_1.
\end{aligned}
$$

Similarly, we have $\|\mathbf{Q}_2\mathbf{Q}_2^\top\|_2 \leq (1+\alpha/C_1)/C_2$. For $\|\mathbf{Q}_1\mathbf{Q}_2^\top\|_2$, similar arguments imply that

$$
\mathbf{Q}_1\mathbf{Q}_2^\top = \mathbb{1}_n \otimes (\boldsymbol{\Lambda}^*)_s^{-1/2}[(\boldsymbol{\Lambda}^*)_t^{-1/2}]^\top \otimes \mathbf{M},
$$

and hence its spectral norm is bounded as

$$
\begin{aligned}
\|\mathbf{Q}_1\mathbf{Q}_2^\top\|_2 &= \left|(\boldsymbol{\Lambda}^*)_s^{-1/2}[(\boldsymbol{\Lambda}^*)_t^{-1/2}]^\top\right| \cdot \|\mathbb{1}_n\|_2\|\mathbf{M}\|_2 \\
&\leq \|\boldsymbol{\Psi}^*\|_2\|\mathbf{M}\|_2 \leq (1+\alpha/C_1)/C_2,
\end{aligned}
$$

where the first inequality is because the above derivation and the Cauchy-Schwarz inequality. Specifically, let $\boldsymbol{\Psi}^* = (\boldsymbol{\Psi}_{i,j}^*)$, we have

$$
\left|(\boldsymbol{\Lambda}^*)_s^{-1/2}[(\boldsymbol{\Lambda}^*)_t^{-1/2}]^\top\right| = \sqrt{(\boldsymbol{\Psi}^*)_s[(\boldsymbol{\Psi}^*)_t]^\top} = \Big[\sum_{j=1}^q \boldsymbol{\Psi}_{s,j}^*\boldsymbol{\Psi}_{t,j}^*\Big]^{1/2}
$$

$$
\leq \Big\{(\sum_{j=1}^q \boldsymbol{\Psi}_{s,j}^{*2})(\sum_{j=1}^q \boldsymbol{\Psi}_{t,j}^{*2})\Big\}^{1/4} \leq \sqrt{\|\boldsymbol{\Psi}^*\|_2\|\boldsymbol{\Psi}^*\|_2} \leq C_2^{-1}.
$$

Applying the same techniques to $\|\mathbf{H}_2\|_2$, we have

$$
\begin{aligned}
\|\mathbf{H}_1\|_2 &\leq 4(1+\alpha/C_1)/C_2, &\text{(B.2)} \\
\|\mathbf{H}_2\|_2 &\leq 4(1+\alpha/C_1)/C_2. &\text{(B.3)}
\end{aligned}
$$

Next, we apply Lemma C.3 to bound the (s,t)-th entry of the differential matrix between the sample-based term and its expectation. Denote $\rho_{s,t} := [p^{-1}\mathbb{E}(\mathbf{X}^\top\boldsymbol{\Omega}\mathbf{X})]_{s,t}$. According to the derivation in (B.1), we have

$$
\begin{aligned}
&\left\{\frac{1}{np}\sum_{i=1}^n \mathbf{X}_i^\top\boldsymbol{\Omega}\mathbf{X}_i - \frac{1}{p}\mathbb{E}(\mathbf{X}^\top\boldsymbol{\Omega}\mathbf{X})\right\}_{s,t} \\
&= \left[\frac{1}{4np}\sum_{i,j}(a_{ij}+b_{ij})^2 - \frac{\boldsymbol{\Delta}_{s,t}+\rho_{s,t}}{2}\right] - \left[\frac{1}{4np}\sum_{i,j}(a_{ij}-b_{ij})^2 - \frac{\boldsymbol{\Delta}_{s,t}-\rho_{s,t}}{2}\right], \text{(B.4)}
\end{aligned}
$$

where $\boldsymbol{\Delta}_{s,t}$ is defined as

$$
\boldsymbol{\Delta}_{s,t} := \mathbb{E}\Big\{(4np)^{-1}\sum_{i,j}[(a_{ij}+b_{ij})^2 + (a_{ij}-b_{ij})^2]\Big\}.
$$

Furthermore, according to the definition of $\rho_{s,t}$ and (B.1), we have $\mathbb{E}\{(4np)^{-1}\sum_{i=1}^n\sum_{j=1}^p[(a_{ij}+b_{ij})^2 - (a_{ij}-b_{ij})^2]\} = \rho_{s,t}$. Therefore, we have

$$
\mathbb{E}\Big\{(4np)^{-1}\sum_{i,j}(a_{ij}+b_{ij})^2\Big\} = \frac{\boldsymbol{\Delta}_{s,t}+\rho_{s,t}}{2}, \tag{B.5}
$$

$$
\mathbb{E}\Big\{(4np)^{-1}\sum_{i,j}(a_{ij}-b_{ij})^2\Big\} = \frac{\boldsymbol{\Delta}_{s,t}-\rho_{s,t}}{2}. \tag{B.6}
$$

Therefore, (B.4) implies that, for any $\delta > 0$,

$$\mathbb{P}\Big[\Big|\Big\{\frac{1}{np}\sum_{i=1}^{n}\mathbf{X}_i^\top\boldsymbol{\Omega}\mathbf{X}_i - \frac{1}{p}\mathbb{E}(\mathbf{X}^\top\boldsymbol{\Omega}\mathbf{X})\Big\}_{s,t}\Big| \geq \delta\Big] \leq$$

$$\underbrace{\mathbb{P}\Big[\Big|\frac{1}{np}\sum_{i,j}(a_{ij}+b_{ij})^2 - 2(\boldsymbol{\Delta}_{s,t}+\rho_{s,t})\Big| > 2\delta\Big]}_{I_1} + \underbrace{\mathbb{P}\Big[\Big|\frac{1}{np}\sum_{i,j}(a_{ij}-b_{ij})^2 - 2(\boldsymbol{\Delta}_{s,t}-\rho_{s,t})\Big| > 2\delta\Big]}_{I_2}.$$

Remind that $\sum_{i=1}^{n}\sum_{j=1}^{p}(a_{ij}+b_{ij})^2 = \text{vec}(\mathbf{A}) + \text{vec}(\mathbf{B}) \sim \text{N}(0;\mathbf{H}_1)$ and $\sum_{i=1}^{n}\sum_{j=1}^{p}(a_{ij}-b_{ij})^2 = \text{vec}(\mathbf{A}) - \text{vec}(\mathbf{B}) \sim \text{N}(0;\mathbf{H}_2)$. According to (B.5) and (B.6), we apply Lemma C.3 to obtain

$$I_1 \leq 2\exp\Big\{-\frac{np}{2}\Big(\frac{\delta}{2\|\mathbf{H}_1\|_2} - \frac{2}{\sqrt{np}}\Big)^2\Big\} + 2\exp(-np/2),$$

$$I_2 \leq 2\exp\Big\{-\frac{np}{2}\Big(\frac{\delta}{2\|\mathbf{H}_2\|_2} - \frac{2}{\sqrt{np}}\Big)^2\Big\} + 2\exp(-np/2).$$

Finally, in order to derive the convergence rate of the maximal difference over all index (s,t), we employ the max sum inequality. That is, for random variables $x_1, \ldots, x_n$, we have $\mathbb{P}(\max_i x_i \geq t) \leq \sum_{i=1}^{n}\mathbb{P}(x_i \geq t) \leq n\max_i \mathbb{P}(x_i \geq t)$. This together with (B.2) and (B.3) imply that

$$\mathbb{P}\Big[\max_{(s,t)}\Big\{\frac{1}{np}\sum_{i=1}^{n}\mathbf{X}_i^\top\boldsymbol{\Omega}\mathbf{X}_i - \frac{1}{p}\mathbb{E}(\mathbf{X}^\top\boldsymbol{\Omega}\mathbf{X})\Big\}_{s,t} \geq \delta\Big]$$

$$\leq 4q^2\exp\Big\{-\frac{np}{2}\Big[\frac{\delta C_1 C_2}{8(C_1+\alpha)} - \frac{2}{\sqrt{np}}\Big]^2\Big\} + 4q^2\exp(-np/2). \tag{B.7}$$

Let $\delta = 8(C_1+\alpha)(C_1 C_2)^{-1}[4\sqrt{\log q/(np)} + 3(np)^{-1/2}]$ in (B.7) which satisfies the condition in Lemma C.3 since $\delta > 2(np)^{-1/2}$ when q is sufficiently large. Therefore, we obtain the desirable conclusion that, with high probability,

$$\max_{(s,t)}\Big\{\frac{1}{np}\sum_{i=1}^{n}\mathbf{X}_i^\top\boldsymbol{\Omega}\mathbf{X}_i - \frac{1}{p}\mathbb{E}(\mathbf{X}^\top\boldsymbol{\Omega}\mathbf{X})\Big\}_{s,t} = O_P\Big(\sqrt{\frac{\log q}{np}}\Big).$$

This ends the proof of Lemma B.1. ∎

Lemma B.2. Assume i.i.d. tensor data $\mathcal{T}, \mathcal{T}_1, \ldots, \mathcal{T}_n \in \mathbb{R}^{m_1 \times m_2 \times \cdots \times m_K}$ follows the tensor normal distribution $\text{TN}(\mathbf{0}; \boldsymbol{\Sigma}_1^*, \ldots, \boldsymbol{\Sigma}_K^*)$. Assume Condition 3.2 holds. For any symmetric and positive definite matrices $\boldsymbol{\Omega}_j \in \mathbb{R}^{m_j \times m_j}, j \neq k$, we have

$$\mathbb{E}[\mathbf{S}_k] = \frac{m_k[\prod_{j\neq k}\text{tr}(\boldsymbol{\Sigma}_j^*\boldsymbol{\Omega}_j)]}{m}\boldsymbol{\Sigma}_k^*,$$

for $\mathbf{S}_k = \frac{m_k}{nm}\sum_{i=1}^{n}\mathbf{V}_i\mathbf{V}_i^\top$ with $\mathbf{V}_i = \big[\mathcal{T}_i \times \{\boldsymbol{\Omega}_1^{1/2}, \ldots, \boldsymbol{\Omega}_{k-1}^{1/2}, \mathbb{1}_{m_k}, \boldsymbol{\Omega}_{k+1}^{1/2}, \ldots, \boldsymbol{\Omega}_K^{1/2}\}\big]_{(k)}$ and $m = \prod_{k=1}^{K} m_k$. Moreover, we have

$$\max_{s,t}\Big\{\mathbf{S}_k - \frac{m_k[\prod_{j\neq k}\text{tr}(\boldsymbol{\Sigma}_j^*\boldsymbol{\Omega}_j)]}{m}\boldsymbol{\Sigma}_k^*\Big\}_{s,t} = O_P\Big(\sqrt{\frac{m_k\log m_k}{nm}}\Big). \tag{B.8}$$

Proof of Lemma B.2: The proof follows by carefully examining the distribution of $\mathbf{V}_i$ and then applying Lemma B.1. We only show the case with $K = 3$ and $k = 1$. The extension to a general K follows similarly.

According to the property of mode-k tensor multiplication, we have $\mathbf{V}_i = [\mathcal{T}_i]_{(1)}(\boldsymbol{\Omega}_3^{1/2} \otimes \boldsymbol{\Omega}_2^{1/2})$, and hence

$$\mathbf{S}_1 = \frac{1}{nm_2m_3}\sum_{i=1}^{n}[\mathcal{T}_i]_{(1)}(\boldsymbol{\Omega}_3^{1/2}\otimes\boldsymbol{\Omega}_2^{1/2})(\boldsymbol{\Omega}_3^{1/2}\otimes\boldsymbol{\Omega}_2^{1/2})[\mathcal{T}_i]_{(1)}^\top$$

$$= \frac{1}{nm_2m_3}\sum_{i=1}^{n}[\mathcal{T}_i]_{(1)}(\boldsymbol{\Omega}_3\otimes\boldsymbol{\Omega}_2)[\mathcal{T}_i]_{(1)}^\top.$$

8

When tensor $\mathcal{T}_i \sim \mathrm{TN}(\mathbf{0}; \boldsymbol{\Sigma}_1^*, \boldsymbol{\Sigma}_2^*, \boldsymbol{\Sigma}_3^*)$, the property of mode-$k$ tensor multiplication shown in Proposition 2.1 in [31] implies that

$$[\mathcal{T}_i]_{(1)} \in \mathbb{R}^{m_1 \times (m_2 m_3)} \sim \mathrm{MN}(\mathbf{0}; \boldsymbol{\Sigma}_1^*, \boldsymbol{\Sigma}_3^* \otimes \boldsymbol{\Sigma}_2^*),$$

where $\mathrm{MN}(\mathbf{0}; \boldsymbol{\Sigma}_1^*, \boldsymbol{\Sigma}_3^* \otimes \boldsymbol{\Sigma}_2^*)$ is the matrix-variate normal [32] such that the row covariance matrix of $[\mathcal{T}_i]_{(1)}$ is $\boldsymbol{\Sigma}_1^*$ and the column covariance matrix of $[\mathcal{T}_i]_{(1)}$ is $\boldsymbol{\Sigma}_3^* \otimes \boldsymbol{\Sigma}_2^*$. Therefore, in order to show (B.8), according to Lemma B.1, it is sufficient to show

$$\mathbb{E}[\mathbf{S}_1] = \frac{\mathrm{tr}(\boldsymbol{\Sigma}_3^* \boldsymbol{\Omega}_3)\mathrm{tr}(\boldsymbol{\Sigma}_2^* \boldsymbol{\Omega}_2)}{m_2 m_3} \boldsymbol{\Sigma}_1^*. \tag{B.9}$$

According to the distribution of $[\mathcal{T}_i]_{(1)}$, we have

$$\mathbf{V}_i \sim \mathrm{MN}\left(\mathbf{0}; \boldsymbol{\Sigma}_1^*, (\boldsymbol{\Omega}_3^{1/2} \otimes \boldsymbol{\Omega}_2^{1/2})(\boldsymbol{\Sigma}_3^* \otimes \boldsymbol{\Sigma}_2^*)(\boldsymbol{\Omega}_3^{1/2} \otimes \boldsymbol{\Omega}_2^{1/2})\right),$$

and hence

$$\mathbf{V}_i^\top \sim \mathrm{MN}\left(\mathbf{0}; (\boldsymbol{\Omega}_3^{1/2} \otimes \boldsymbol{\Omega}_2^{1/2})(\boldsymbol{\Sigma}_3^* \otimes \boldsymbol{\Sigma}_2^*)(\boldsymbol{\Omega}_3^{1/2} \otimes \boldsymbol{\Omega}_2^{1/2}), \boldsymbol{\Sigma}_1^*\right).$$

Therefore, according to Lemma C.1, we have

$$\mathbb{E}[\mathbf{V}_i \mathbf{V}_i^\top] = \boldsymbol{\Sigma}_1^* \mathrm{tr}\left[(\boldsymbol{\Omega}_3 \otimes \boldsymbol{\Omega}_2)(\boldsymbol{\Sigma}_3^* \otimes \boldsymbol{\Sigma}_2^*)\right] = \boldsymbol{\Sigma}_1^* \mathrm{tr}(\boldsymbol{\Sigma}_3^* \boldsymbol{\Omega}_3)\mathrm{tr}(\boldsymbol{\Sigma}_2^* \boldsymbol{\Omega}_2),$$

which implies (B.9) according to the definition of $\mathbf{S}_1$. Finally, applying Lemma B.1 to $\mathbf{S}_1$ leads to the desirable result. This ends the proof of Lemma B.2. ∎

The following lemma establishes the rate of convergence of the sample covariance matrix in max norm.

Lemma B.3. Assume i.i.d. tensor data $\mathcal{T}, \mathcal{T}_1, \ldots, \mathcal{T}_n \in \mathbb{R}^{m_1 \times m_2 \times \cdots \times m_K}$ follows the tensor normal distribution $\mathrm{TN}(\mathbf{0}; \boldsymbol{\Sigma}_1^*, \cdots, \boldsymbol{\Sigma}_K^*)$, and assume Condition 3.2 holds. Let $\widehat{\boldsymbol{\Omega}}_j \in \mathbb{R}^{m_j \times m_j}, j \neq k$, be the estimated precision matrix from Algorithm 1 with iteration number $T = 1$. Denote the k-th sample covariance matrix as

$$\widehat{\mathbf{S}}_k = \frac{m_k}{nm} \sum_{i=1}^{n} \widehat{\mathbf{V}}_i \widehat{\mathbf{V}}_i^\top,$$

with $m = \prod_{k=1}^{K} m_k$ and $\widehat{\mathbf{V}}_i := \left[\mathcal{T}_i \times \{\widehat{\boldsymbol{\Omega}}_1^{1/2}, \ldots, \widehat{\boldsymbol{\Omega}}_{k-1}^{1/2}, \mathbb{1}_{m_k}, \widehat{\boldsymbol{\Omega}}_{k+1}^{1/2}, \ldots, \widehat{\boldsymbol{\Omega}}_K^{1/2}\}\right]_{(k)}$. We have

$$\max_{s,t} \left[\widehat{\mathbf{S}}_k - \boldsymbol{\Sigma}_k^*\right]_{s,t} = O_P\left(\max_{j=1,\ldots,K} \sqrt{\frac{(m_j + s_j)\log m_j}{nm}}\right). \tag{B.10}$$

Proof of Lemma B.3: The proof follows by decomposing the $\widehat{\mathbf{S}}_k - \boldsymbol{\Sigma}_k^*$ into two parts and then applying Lemma B.2 and Theorem 3.5 for each part to bound the final error.

Note that the triangle inequality implies that

$$\left\|\widehat{\mathbf{S}}_k - \boldsymbol{\Sigma}_k^*\right\|_\infty \leq \underbrace{\left\|\widehat{\mathbf{S}}_k - \frac{m_k[\prod_{j \neq k}\mathrm{tr}(\boldsymbol{\Sigma}_j^* \widehat{\boldsymbol{\Omega}}_j)]}{m}\boldsymbol{\Sigma}_k^*\right\|_\infty}_{I_1} + \underbrace{\left\|\frac{m_k[\prod_{j \neq k}\mathrm{tr}(\boldsymbol{\Sigma}_j^* \widehat{\boldsymbol{\Omega}}_j)]}{m}\boldsymbol{\Sigma}_k^* - \boldsymbol{\Sigma}_k^*\right\|_\infty}_{I_2}.$$

Note that here the covariance matrix $\widehat{\mathbf{S}}_k$ is constructed based on the estimators $\widehat{\boldsymbol{\Omega}}_j, j \neq k$. According to (B.8) in Lemma B.2, we have

$$I_1 = O_P\left(\sqrt{\frac{m_k \log m_k}{nm}}\right).$$

The remainder part is to bound the error I_2. Note that $\mathrm{tr}(\boldsymbol{\Sigma}_j^* \boldsymbol{\Omega}_j^*) = \mathrm{tr}(\mathbb{1}_{m_j}) = m_j$. Therefore,

$$I_2 = \underbrace{\left|\frac{m_k}{m}\left[\prod_{j \neq k}\mathrm{tr}(\boldsymbol{\Sigma}_j^* \widehat{\boldsymbol{\Omega}}_j) - \prod_{j \neq k}\mathrm{tr}(\boldsymbol{\Sigma}_j^* \boldsymbol{\Omega}_j^*)\right]\right|}_{I_3} \|\boldsymbol{\Sigma}_k^*\|_\infty.$$

Given that $\|\mathbf{\Sigma}_k^*\|_\infty = O_P(1)$, it is sufficient to bound the coefficient I_3. We only demonstrate the proofs with $K = 3$ and $k = 1$. The extension to a general K follows similarly. In this case, we have

$$
\begin{aligned}
I_3 &= \frac{m_1}{m}\left|\mathrm{tr}(\mathbf{\Sigma}_2^*\widehat{\mathbf{\Omega}}_2)\mathrm{tr}(\mathbf{\Sigma}_3^*\widehat{\mathbf{\Omega}}_3) - \mathrm{tr}(\mathbf{\Sigma}_2^*\mathbf{\Omega}_2^*)\mathrm{tr}(\mathbf{\Sigma}_3^*\mathbf{\Omega}_3^*)\right| \\
&\leq \left|\frac{\mathrm{tr}(\mathbf{\Sigma}_2^*\widehat{\mathbf{\Omega}}_2)\mathrm{tr}[\mathbf{\Sigma}_3^*(\widehat{\mathbf{\Omega}}_3 - \mathbf{\Omega}_3^*)]}{m_2 m_3}\right| + \left|\frac{\mathrm{tr}[\mathbf{\Sigma}_2^*(\widehat{\mathbf{\Omega}}_2 - \mathbf{\Omega}_2^*)]\mathrm{tr}(\mathbf{\Sigma}_3^*\mathbf{\Omega}_3^*)}{m_2 m_3}\right|.
\end{aligned}
$$

According to the proof of Theorem 3.5, we have $C_1 \leq \mathrm{tr}(\mathbf{\Sigma}_j^*\mathbf{\Omega}_j)/m_j \leq 1/C_1$ for any $j = 1, \ldots, K$ and some constant $C_1 > 0$. Moreover, we have $\mathrm{tr}(\mathbf{\Sigma}_3^*\mathbf{\Omega}_3^*) = m_3$. Therefore, we have

$$
I_3 \leq \left|\frac{\mathrm{tr}[\mathbf{\Sigma}_3^*(\widehat{\mathbf{\Omega}}_3 - \mathbf{\Omega}_3^*)]}{m_3}\right| + \left|\frac{\mathrm{tr}[\mathbf{\Sigma}_2^*(\widehat{\mathbf{\Omega}}_2 - \mathbf{\Omega}_2^*)]}{m_2}\right|.
$$

Here $\mathrm{tr}[\mathbf{\Sigma}_j^*(\widehat{\mathbf{\Omega}}_j - \mathbf{\Omega}_j^*)] \leq \|\mathbf{\Sigma}_j^*\|_F\|\widehat{\mathbf{\Omega}}_j - \mathbf{\Omega}_j^*\|_F \leq \sqrt{m_j}\|\mathbf{\Sigma}_j^*\|_2\|\widehat{\mathbf{\Omega}}_j - \mathbf{\Omega}_j^*\|_F$. According to Condition 3.2, $\|\mathbf{\Sigma}_j^*\|_2 = O_P(1)$. This together with Theorem 3.5 implies that

$$
I_3 = O_P\left(\sqrt{\frac{(m_3 + s_3)\log m_3}{nm}} + \sqrt{\frac{(m_2 + s_2)\log m_2}{nm}}\right).
$$

By generalizing it to a general K and k, we have that

$$
I_3 = O_P\left(\max_{j \neq k}\sqrt{\frac{(m_j + s_j)\log m_j}{nm}}\right),
$$

and hence

$$
\|\widehat{\mathbf{S}}_k - \mathbf{\Sigma}_k^*\|_\infty = O_P\left(\sqrt{\frac{m_k \log m_k}{nm}} + \max_{j \neq k}\sqrt{\frac{(m_j + s_j)\log m_j}{nm}}\right),
$$

which leads to the desirable result. This ends the proof of Lemma B.3. ∎

C   Auxiliary lemmas

Lemma C.1. Assume a random matrix $\mathbf{X} \in \mathbb{R}^{p \times q}$ follows the matrix-variate normal distribution such that $\mathrm{vec}(\mathbf{X}) \sim \mathrm{N}(\mathbf{0}; \mathbf{\Psi}^* \otimes \mathbf{\Sigma}^*)$ with $\mathbf{\Psi}^* \in \mathbb{R}^{q \times q}$ and $\mathbf{\Sigma}^* \in \mathbb{R}^{p \times p}$. Then for any symmetric and positive definite matrix $\mathbf{\Omega} \in \mathbb{R}^{p \times p}$, we have $\mathbb{E}(\mathbf{X}^\top \mathbf{\Omega} \mathbf{X}) = \mathbf{\Psi}^* \mathrm{tr}(\mathbf{\Omega}\mathbf{\Sigma}^*)$.

Proof of Lemma C.1: Since the matrix $\mathbf{\Omega}$ is symmetric and positive definite, it has the Cholesky decomposition $\mathbf{\Omega} = \mathbf{V}^\top \mathbf{V}$, where $\mathbf{V}$ is upper triangular with positive diagonal entries. Let $\mathbf{Y} := \mathbf{V}\mathbf{X}$ and denote the j-th row of matrix $\mathbf{Y}$ as $\mathbf{y}_j = (y_{j,1}, \ldots, y_{j,q})$. We have $\mathbb{E}(\mathbf{X}^\top \mathbf{\Omega}\mathbf{X}) = \mathbb{E}(\mathbf{Y}^\top\mathbf{Y}) = \sum_{j=1}^p \mathbb{E}(\mathbf{y}_j^\top \mathbf{y}_j)$. Here $\mathbf{y}_j = \mathbf{v}_j\mathbf{X}$ with $\mathbf{v}_j$ the j-th row of $\mathbf{V}$. Denote the i-th column of matrix $\mathbf{X}$ as $\mathbf{x}_{(i)}$, we have $y_{j,i} = \mathbf{v}_j\mathbf{x}_{(i)}$. Therefore, the (s, t)-th entry of $\mathbb{E}(\mathbf{y}_j^\top \mathbf{y}_j)$ is

$$
\left[\mathbb{E}(\mathbf{y}_j^\top \mathbf{y}_j)\right]_{(s,t)} = \mathbb{E}[\mathbf{v}_j\mathbf{x}_{(s)}\mathbf{v}_j\mathbf{x}_{(t)}] = \mathbf{v}_j\mathbb{E}[\mathbf{x}_{(s)}\mathbf{x}_{(t)}^\top]\mathbf{v}_j^\top = \mathbf{v}_j\mathbf{\Psi}_{s,t}^*\mathbf{\Sigma}^*\mathbf{v}_j^\top,
$$

where $\mathbf{\Psi}_{s,t}^*$ is the (s, t)-th entry of $\mathbf{\Psi}^*$. The last equality is due to $\mathrm{vec}(\mathbf{X}) = (\mathbf{x}_{(1)}^\top, \ldots, \mathbf{x}_{(q)}^\top)^\top \sim \mathrm{N}(\mathbf{0}; \mathbf{\Psi}^* \otimes \mathbf{\Sigma}^*)$ Therefore, we have

$$
\mathbb{E}(\mathbf{X}^\top\mathbf{\Omega}\mathbf{X}) = \sum_{j=1}^p \mathbb{E}(\mathbf{y}_j^\top\mathbf{y}_j) = \mathbf{\Psi}^*\sum_{j=1}^p \mathbf{v}_j\mathbf{\Sigma}^*\mathbf{v}_j^\top = \mathbf{\Psi}^*\mathrm{tr}\left(\sum_{j=1}^p \mathbf{v}_j^\top\mathbf{v}_j\mathbf{\Sigma}^*\right) = \mathbf{\Psi}^*\mathrm{tr}(\mathbf{\Omega}\mathbf{\Sigma}^*).
$$

This ends the proof of Lemma C.1. ∎

The following lemma is stated by [24].

Lemma C.2. Let random variables $x_1, \ldots, x_n \in \mathbb{R}$ be i.i.d. drawn from standard normal $\mathrm{N}(0;1)$ and denote $\mathbf{x} = (x_1, \ldots, x_n)^\top \in \mathbb{R}^n$ be a random vector. For a function $f : \mathbb{R}^n \to \mathbb{R}$ with Lipschitz constant L, that is, for any vectors $\mathbf{v}_1, \mathbf{v}_2 \in \mathbb{R}^n$, there exists $L \geq 0$ such that $|f(\mathbf{v}_1) - f(\mathbf{v}_2)| \leq L\|\mathbf{v}_1 - \mathbf{v}_2\|_2$. Then, for any $t > 0$, we have

$$\mathbb{P}\left\{|f(\mathbf{x}) - \mathbb{E}[f(\mathbf{x})]| > t\right\} \leq 2\exp\left(-\frac{t^2}{2L^2}\right).$$

The following lemma is useful for the proof of Lemma B.1. A similar statement was given in Lemma I.2 of [33].

Lemma C.3. Suppose that a d-dimensional Gaussian random vector $\mathbf{y} \sim \mathrm{N}(0;\mathbf{Q})$, Then, for any $t > 2/\sqrt{d}$, we have

$$\mathbb{P}\left[\frac{1}{d}\big|\|\mathbf{y}\|_2^2 - \mathbb{E}(\|\mathbf{y}\|_2^2)\big| > 4t\|\mathbf{Q}\|_2\right] \leq 2\exp\left\{-\frac{d\left(t - 2/\sqrt{d}\right)^2}{2}\right\} + 2\exp(-d/2).$$

Proof of Lemma C.3: Note that $\mathbb{E}(\|\mathbf{y}\|_2^2) \leq [\mathbb{E}(\|\mathbf{y}\|_2)]^2$ and hence

$$\|\mathbf{y}\|_2^2 - \mathbb{E}(\|\mathbf{y}\|_2^2) \leq [\|\mathbf{y}\|_2 - \mathbb{E}(\|\mathbf{y}\|_2)][\|\mathbf{y}\|_2 + \mathbb{E}(\|\mathbf{y}\|_2)].$$

The term $(\|\mathbf{y}\|_2 - \mathbb{E}(\|\mathbf{y}\|_2)$ can be bounded via the concentration inequality in Lemma C.2 by noting that $\|\mathbf{y}\|_2$ is a Lipschitz function of Gaussian random vector $\mathbf{y}$. The term $\|\mathbf{y}\|_2 + \mathbb{E}(\|\mathbf{y}\|_2)$ can also be bounded by the large deviation bound since $\mathbf{y}$ is a Gaussian random vector. This ends the proof of Lemma C.3. ∎

D   Additional simulation results

In this section, we explain the details in generating the true precision matrices and then show additional numerical results.

Triangle: For each $k = 1, \ldots, K$, we construct the covariance matrix $\boldsymbol{\Sigma}_k \in \mathbb{R}^{m_k \times m_k}$ such that its (i, j)-th entry is $[\boldsymbol{\Sigma}_k]_{i,j} = \exp(-|h_i - h_j|/2)$ with $h_1 < h_2 < \cdots < h_{m_k}$. The difference $h_i - h_{i-1}$ with $i = 2, \ldots, m_k$ is generated independently and identically from $\mathrm{Unif}(0.5, 1)$. This generated covariance matrix mimics the autoregressive process of order one, i.e., AR(1). We set $\boldsymbol{\Omega}_k^* = \boldsymbol{\Sigma}_k^{-1}$.

Nearest neighbor: For each $k = 1, \ldots, K$, we construct the precision matrix $\boldsymbol{\Omega}_k \in \mathbb{R}^{m_k \times m_k}$ directly from a four nearest-neighbor network. We first randomly pick m_k points from a unit square and compute all pairwise distances among the points. We then search for the four nearest-neighbors of each point and a pair of symmetric entries in the precision matrix $\boldsymbol{\Omega}_k$ that has a random chosen value from $[-1, -0.5] \cup [0.5, 1]$. To ensure its positive definite property, we let the final precision matrix as $\boldsymbol{\Omega}_k^* = \boldsymbol{\Omega}_k + (|\lambda_{\min}(\boldsymbol{\Omega}_k) + 0.2| \cdot \mathbb{1}_{m_k})$, where $\lambda_{\min}(\cdot)$ refers to the smallest eigenvalue.

The additional error criterions for comparison are the averaged estimation errors in Frobinusm norm and max norm, i.e.,

$$\frac{1}{K}\sum_{k=1}^K \big\|\widehat{\boldsymbol{\Omega}}_k - \boldsymbol{\Omega}_k^*\big\|_F, \quad \frac{1}{K}\sum_{k=1}^K \big\|\widehat{\boldsymbol{\Omega}}_k - \boldsymbol{\Omega}_k^*\big\|_\infty.$$

Note that these two criterions are only available to the P-MLE method and our Tlasso. The direct Glasso method estimate the whole Kronecker product and hence could not produce the estimator for each precision matrix.

Remind that, as we show in Theorem 3.5 and Theorem 3.9, the estimation error for the k-th precision matrix is $O_p(\sqrt{m_k(m_k + s_k)\log m_k/(nm)})$ in Frobenius norm or $O_p(\sqrt{m_k \log m_k/(nm)})$ in max norm, where $m = m_1 m_2 m_3$ in this example. These theoretical findings are supported by the numerical results in Figure 2. In particular, as sample size n increases from Scenario s1 to s2, the estimation errors in both Frobenius norm and max norm expectedly decrease. From Scenario s1 to s3, one dimension m_1 increases from 10 to 100, and other dimensions m_2, m_3 decrease from 10 to 5, in which case the averaged estimation error in max norm is decreasing, while the error in Frobenius norm increases due to its additional $\sqrt{m_k + s_k}$ effect. Moreover, compared to the P-MLE
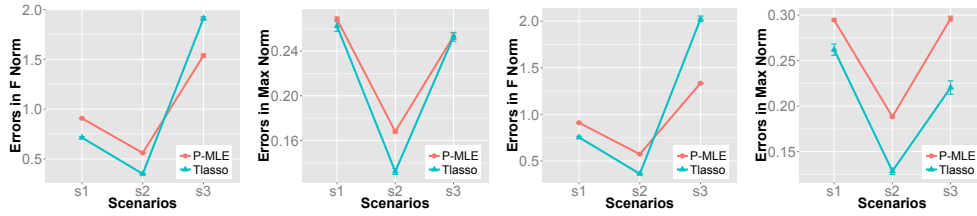
Figure 2: Averaged estimation errors of the precision matrices in Frobenius norm and max norm of each method in Simulations 1&2, respectively. The left two plots are for Simulation 1, and the right two are for Simulation 2.

method, our Tlasso is better in Scenarios s1 and s2 and is worse in Scenario s3 in Frobenius norm. However, in terms of the max norm, our Talsso delivers significant better performance in 4 scenarios and comparable results in the rest 2 scenarios.

References

[1] S. Rendle and L. Schmidt-Thieme. Pairwise interaction tensor factorization for personalized tag recommendation. In *International Conference on Web Search and Data Mining*, 2010.

[2] G.I. Allen. Sparse higher-order principal components analysis. In *International Conference on Artificial Intelligence and Statistics*, 2012.

[3] J. Zahn, S. Poosala, A. Owen, D. Ingram, et al. AGEMAP: A gene expression database for aging in mice. *PLOS Genetics*, 3:2326–2337, 2007.

[4] T. Cai, W. Liu, and H.H. Zhou. Estimating sparse precision matrix: Optimal rates of convergence and adaptive estimation. *Annals of Statistics*, 2015.

[5] C. Leng and C.Y. Tang. Sparse matrix graphical models. *Journal of the American Statistical Association*, 107:1187–1200, 2012.

[6] J. Yin and H. Li. Model selection and estimation in the matrix normal graphical model. *Journal of Multivariate Analysis*, 107:119–140, 2012.

[7] T. Tsiligkaridis, A. O. Hero, and S. Zhou. On convergence of Kronecker graphical Lasso algorithms. *IEEE Transactions on Signal Processing*, 61:1743–1755, 2013.

[8] S. Zhou. Gemini: Graph estimation with matrix variate normal instances. *Annals of Statistics*, 42:532–562, 2014.

[9] S. He, J. Yin, H. Li, and X. Wang. Graphical model selection and estimation for high dimensional tensor data. *Journal of Multivariate Analysis*, 128:165–185, 2014.

[10] P. Jain, P. Netrapalli, and S. Sanghavi. Low-rank matrix completion using alternating minimization. In *Symposium on Theory of Computing*, pages 665–674, 2013.

[11] P. Netrapalli, P. Jain, and S. Sanghavi. Phase retrieval using alternating minimization. In *Advances in Neural Information Processing Systems*, pages 2796–2804, 2013.

[12] J. Sun, Q. Qu, and J. Wright. Complete dictionary recovery over the sphere. *arXiv:1504.06785*, 2015.

[13] S. Arora, R. Ge, T. Ma, and A. Moitra. Simple, efficient, and neural algorithms for sparse coding. *arXiv:1503.00778*, 2015.

[14] A. Anandkumar, R. Ge, D. Hsu, S. Kakade, and M. Telgarsky. Tensor decompositions for learning latent variable models. *Journal of Machine Learning Research*, 15:2773–2832, 2014.

[15] W. Sun, J. Lu, H. Liu, and G. Cheng. Provable sparse tensor decomposition. *arXiv:1502.01425*, 2015.

[16] S. Zhe, Z. Xu, X. Chu, Y. Qi, and Y. Park. Scalable nonparametric multiway data analysis. In *International Conference on Artificial Intelligence and Statistics*, 2015.

[17] S. Zhe, Z. Xu, Y. Qi, and P. Yu. Sparse bayesian multiview learning for simultaneous association discovery and diagnosis of alzheimer's disease. In *Twenty-Ninth AAAI Conference on Artificial Intelligence*, 2015.

[18] T. Kolda and B. Bader. Tensor decompositions and applications. *SIAM Review*, 51:455–500, 2009.

[19] R. Tibshirani. Regression shrinkage and selection via the Lasso. *Journal of the Royal Statistical Society, Series B*, 58:267–288, 1996.

[20] M. Yuan and Y. Lin. Model selection and estimation in the gaussian graphical model. *Biometrika*, 94:19–35, 2007.

[21] J. Friedman, H. Hastie, and R. Tibshirani. Sparse inverse covariance estimation with the graphical Lasso. *Biostatistics*, 9:432–441, 2008.

[22] A. J. Rothman, P. J. Bickel, E. Levina, and J. Zhu. Sparse permutation invariant covariance estimation. *Electronic Journal of Statistics*, 2:494–515, 2008.

[23] W. Sun, J. Wang, and Y. Fang. Consistent selection of tuning parameters via variable selection stability. *Journal of Machine Learning Research*, 14:3419–3440, 2013.

[24] M. Ledoux and M. Talagrand. *Probability in Banach Spaces: Isoperimetry and Processes*. Springer, 2011.

[25] J. Fan, Y. Feng, and Y. Wu. Network exploration via the adaptive Lasso and scad penalties. *Annals of Statistics*, 3:521–541, 2009.

[26] P. Zhao and B. Yu. On model selection consistency of Lasso. *Journal of Machine Learning Research*, 7:2541–2567, 2006.

[27] P. Ravikumar, M.J. Wainwright, G. Raskutti, and B. Yu. High-dimensional covariance estimation by minimizing ℓ_1-penalized log-determinant divergence. *Electronic Journal of Statistics*, 5:935–980, 2011.

[28] Z. Wang, H. Liu, and T. Zhang. Optimal computational and statistical rates of convergence for sparse nonconvex learning problems. *Annals of Statistics*, 42:2164–2201, 2014.

[29] T. Zhao, H. Liu, K. Roeder, J. Lafferty, and L. Wasserman. The huge package for high-dimensional undirected graph estimation in R. *Journal of Machine Learning Research*, 13:1059–1062, 2012.

[30] A. Gupta and D. Nagar. *Matrix variate distributions*. Chapman and Hall/CRC Press, 2000.

[31] P. Hoff. Separable covariance arrays via the Tucker product, with applications to multivariate relational data. *Bayesian Analysis*, 6:179–196, 2011.

[32] A.P. Dawid. Some matrix-variate distribution theory: Notational considerations and a bayesian application. *Biometrika*, 68:265–274, 1981.

[33] S. Negahban and M.J. Wainwright. Estimation of (near) low-rank matrices with noise and high-dimensional scaling. *Annals of Statistics*, 39:1069–1097, 2011.